UNIVERSITÉ DE NANTES

Diplôme d'Université de Gemmologie

EXPERIMENTAL DISSERTATION

Brief Study On Zambian Emerald Inclusions

By
Ms. Deepa Srinivasa
Batch of 2017-18

ACADEMIC GUIDANCE
Prof. Fritsch
Dr. Rondeau
Université de Nantes
U.F.R. Sciences et Techniques

Table Of Contents

1. Introduction

This dissertation was written as part of the Experimental Research for Diplôme d'Université en Gemmologie DUG, Nantes, France. The objective of attending this Diplome program was to enhance my knowledge in learning to work with advanced equipment as well as to research the subject in-depth.

Gemstones always fascinated me and my quest for gaining advanced knowledge of Gemstones remains unabated. The field of study of Gemstones offered so much to see and learn, enabling for me a very satisfying journey with never a dull moment. From the external beauty to the intimate beauty of gemstone inclusions, from gem lore to the mines, the people and the landscapes gems originate from, be it color or inclusions or origin, every aspect captivates me.

Inspiration was drawn from the field visits to mines and markets, meeting miners from producing countries, laboratory technicians, leading gemologists like Vincent Pardieu, Edward Boehm and many others who inspired and drew me closer to gemstones and their mysterious origins. Origin determination being a vast topic and with the limited time and conditions, as advised and suggested by Professor Dr. Emmanuel Fritsch, I chose to concentrate on "Inclusions in Zambian Emerald's" to be my dissertation.

Emerald's lush green has soothed souls and excited imaginations since antiquity. With a variety of inclusions emeralds host, often called "Jardin", these imperfections while beautiful are unique to each emerald, and it was always intriguing to find something different in every deposit. Whilst majority of the emeralds traded are Zambian and the only emerald samples that I could get for study happened to be Zambian (as stated by donor), I was delighted to study these and present my findings as part of this dissertation.

1a. Brief History of Emeralds from Around the World

Emeralds have been mined since the inception of 1500 BC in Egypt, India and Austria. World's largest producer of emeralds lies in Colombia, constituting 50– 95% of the world generation being dependent and varying with year, source and grade. The production has gone up by 78% from 2000 to 2010. Muzo, Coscuez, and Chivor are the three fundamental mining zones in Colombia. The rarest "trapiche" emeralds are found in Colombia characterized by ray-like spokes of dark impurities.

Zambia is the world's second greatest maker, with its Kafubu River region deposits (Kagem Mines) around 45 km (28 mi) southwest of Kitwe. In 2004 it produced 20% of the world's precious stones and in 2011 the Kagem mines delivered 3.74 tons of emeralds.

Emeralds are discovered everywhere throughout the world in nations, for example, Afghanistan, Australia, Austria, Brazil, Bulgaria, Cambodia, Canada, China, Egypt, Ethiopia, France, Germany, India, Italy, Kazakhstan, Madagascar, Mozambique, Namibia, Nigeria, Norway, Pakistan, Russia, Somalia, South Africa, Spain, Switzerland, Tanzania, the United States, Zambia, and Zimbabwe. In the US, emeralds have been found in Connecticut, Montana, Nevada, North Carolina, and South Carolina. In Canada, in 1997 emeralds were found in the Yukon.[13]

1b. Brief History Of Zambian Emeralds

Zambia is viewed as the world's second most source of high quality emeralds only next to Colombia with deposits close to the Kafubu River in the Ndola Rural Restricted Area. Though since 1928 emeralds have been found in this area but mass production started only in 1970s. By 2004, large extent of emeralds was being mined from extensive open-pit activities at the Kagem, Grizzly, and Chantete concessions.

Emerald have mineralized mostly in phlogopite zones neighboring Be-bearing quartz-tourmaline veins that metasomatically changed Cr-bearing metabasite rocks. Most of the rough is cut in India and Israel. Zambian emeralds have moderately high R.I. and S.G. values, with inclusions comprising of mostly healed fissures, and actinolite, phlogopite, dravite, fluorapatite, magnetite, and hematite. *(table:1)* They contain moderate amount of Cr, Mg, and Na with high amounts of Fe content, and generally higher Cs and Li. While Zambian emeralds are practically identical to those from other commercially essential areas, by and large they might be isolated by a mix of their physical properties, magnification and chemical composition. [6]

Emeralds were initially discovered in 1928 in Kafubu by Rhodesia Congo Border Concession Company (RCBCC) which came to be known as Miku mine (Sliwa and Nguluwe, 1984; Seifert et al., 2004). Experimental work continued in 1940s and 1950s by the Rhokana Company and by Rio Tinto Mineral Search of Africa company though the early productions were minimal. Zambian government later declared the area as "restricted zone" due to irradical illegal mining. [14]

Fig:1- Map of Africa showing gem producing areas. [15]

In lieu of the above sanctions by the Zambian government only government sanctioned mining was allowed by both large scale and small-scale miners. Later in 1980 Kagem Mining Ltd was given permission to mine Kafubu deposits. Systematic mining began in Pirala in 2004 by UK based company Gemfields Resource PLC which is 55% owned by Johannesburg's Pallinghurst Resources. Gemfields gained 100% control of the two mines in the area about 60% of emerald bearing rocks in Ndola Rural Emerald Restricted area. By 2007 Gemfields was given the management contract for Kagem mine which later acquired 75% ownership.
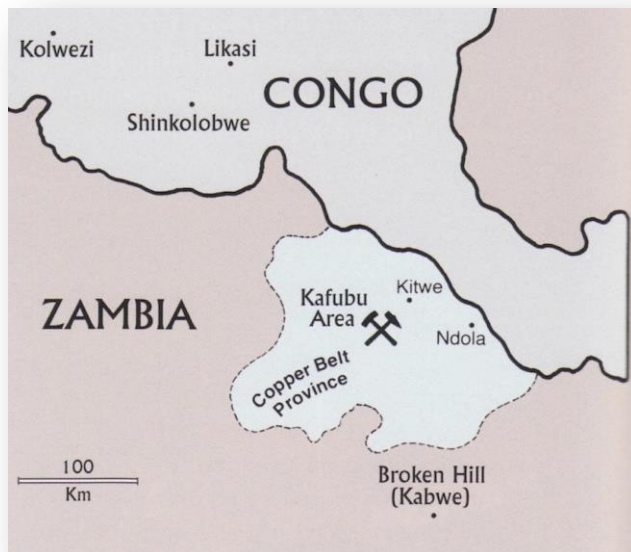
Fig:2- Map of Zambia showing major Emerald producing mine- Kafubu. [14]

Kagem mine is known as the largest open -pit mine for colored stones. It covers an area of a roughly 1sq km and has about 400 men working with a total production of $15 million to $30 million. Due to unviable underground operations all operations have been made open-pit. [14]
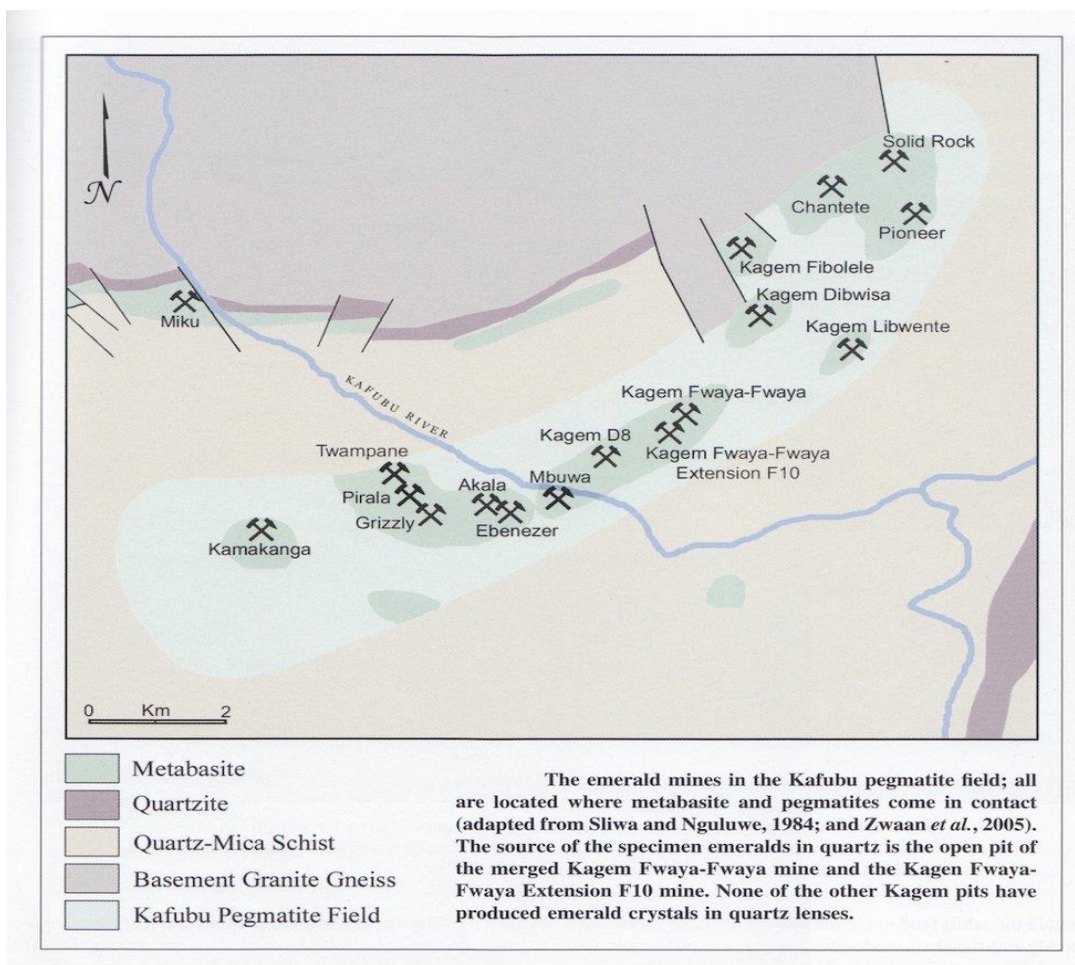

The emerald mines in the Kafubu pegmatite field; all are located where metabasite and pegmatites come in contact (adapted from Sliwa and Nguluwe, 1984; and Zwaan *et al.*, 2005). The source of the specimen emeralds in quartz is the open pit of the merged Kagem Fwaya-Fwaya mine and the Kagen Fwaya-Fwaya Extension F10 mine. None of the other Kagem pits have produced emerald crystals in quartz lenses.

Legend:
- Metabasite
- Quartzite
- Quartz-Mica Schist
- Basement Granite Gneiss
- Kafubu Pegmatite Field

Fig:3- The map shows the emerald mines in the Kafubu pegmatite field that are all located where metabasite and pegmatites come in contact. [14]

1c. Geology of Zambian Emeralds:

Fig:4- The image shows Emerald bearing pegmatite bands intruding amphibolite and talc-magnetite schist. [14]

The Metamorphic Muva Supergroup which is 1.7-billion-year-old forms the three major rock units in Kagem mine area. Mica schist forms the topmost layer and about 30-40 meters in thickness. About 20 meters is weathered into soil and laterite. Under this layer is present a layer of amphibolite of 15 and 20 meters thickness. Metabasite forms the next layer which is rich in magnesium and chromium metamorphosed volcanic rocks talc-chlorite-actinolite schist +- magnetite, which hosts the emerald mineralization (Sliwa and Nguluwe, 1984; Seifert et al., 2004).

Light-shaded beryllium-bearing quartz-feldspar pegmatite's and epigenetic aqueous quartz-rich veins related with the Pan-African Orogeny cut from the three units. Asper the Potassium/argon age-dating of muscovite related with emerald precious stones in the zones shows crystallization happened 447-452 million years back (Seifert et al., 2004). [14]

The Zambian Copperbelt and Kafubu area contain a very multifaceted collection of geologic units which developed amid three progressive orogenies of Proterozoic age. (i.e., mountain-building events ranging from about 2 billion to 500 million years ago [My]). The emerald deposits are facilitated by metamorphic rocks of the Muva Supergroup (Daly and Unrug, 1983) that overlay the basement granite stone gneisses along a structural unconformity. The Muva rocks comprise of quartzite's, mica schists, and metabasites. [6]

Emerald mineralization is facilitated by the metabasites, which comprise of powder chlorite-actinolite ± magnetite schists (Hickman 1973; Sliwa and Nguluwe, 1984).

These schists are thought to signify metamorphosed volcanic rocks that were mostly surpassed by komatiites (i.e., very magnesian ultramafic rocks; Seifert et al., 2004c). High chromium content is responsible for emerald mineralization. [6]

Pegmatites and beryllium rich granites intruded various crustal units in central and NW Zambia during the late Pan African orogeny. Field studies at various mines and pits in Kafubu specify the existence of large beryllium bearing pegmatite's fields and hydrothermal veins for 20 km long. This area covers significant horizons of metabasites which are enhanced in chromium bringing about emerald mineralization. Potassium-argon dating of muscovite from a pegmatite and a related quartz-tourmaline vein gave cooling ages of 447– 452 My (Seifert et al., 2004c). This compares to the surmised time of emerald mineralization, when the stones cooled beneath 350 ± 50°C (which is the rough temperature at which muscovite moves toward becoming "closed" to argon misfortune. [6]

1d. Typical Gemological Properties of Zambian Emeralds:

Color	Colors range from light to dark green to slightly bluish to bluish green; typically a saturated bluish green with a medium to medium-dark tone
Clarity	Very slightly to heavily included
Refractive indices	$n_o = 1.585–1.599$; $n_e = 1.578–1.591$
	$n_o = 1.589–1.597$; $n_e = 1.581–1.589^b$
	$n_o = 1.602$; $n_e = 1.592^c$
Birefringence	$0.006–0.009$ (0.008^b, 0.010^c)
Optic character	Uniaxial negative
Specific gravity	2.71–2.78
	$2.69–2.77^b$
Pleochroism	Strong yellowish green (o-ray) and bluish green (e-ray); some stones showed strong greenish yellow (o-ray) and greenish blue (e-ray)
Fluorescence	Usually inert to long- and short-wave UV radiation; sometimes faint green to long-wave
Chelsea filter reaction	No reaction or light pink to red (deep green samples)
Absorption spectrum	Absorption between 580 and 630 nm; distinct lines at approximately 636, 662, and 683 nm
Internal features	• "Feathers" in flat, curved, (rarely) conchoidal forms or undulatory/scalloped shapes • Partially healed fissures with various shapes of two- and three-phase fluid inclusions, but typically equant or rectangular • Isolated negative crystals containing CO_2 and CH_4 • Parallel oriented decrepitated inclusions appearing as silvery disks or brownish spots, depending on the lighting • Mineral inclusions (this study): randomly oriented actinolite needles, platelets of phlogopite or rare chlorite, equant to columnar dravite, fluorapatite, magnetite, hematite, chlorite, quartz, fluorite; carbonates (magnesite/siderite, ferroan dolomite, ankerite and calcite); niobian rutile, pyrite, talc, zircon, barite, albite, calcite, sphene (titanite), and beryl • Characteristic inclusions described by other authors: phlogopite/biotite, actinolite-tremolite, and square and rectangular-shaped fluid inclusions (Milisenda et al., 1999); phlogopite, glauconite, talc, apatite, quartz, and Fe-Mn and Fe-Cr oxides (Moroz and Eliezri, 1999); apatite, quartz, chrysoberyl, margarite, muscovite, and rutile or brookite (Graziani et al., 1983); tourmaline, limonite, magnetite, mica, rutile, hematite, and apatite (Koivula, 1982; 1984), and also chrysotile (Gübelin and Koivula, 1986) • Cavities, representing dissolved columnar mineral inclusions

Table: 1 - Physical properties of emeralds from the Kafubu area, Zambia [6]

2. Materials & Methods

For this study, I examined a total of 8 emeralds ranging between 1.06-3.69 carats, of which 7 were oval faceted and 1 was faceted emerald cut. 1 out of the 7 ovals was flat. All the samples were transparent and these samples were loaned out from a friend who informed these samples were Zambian origin. Most of the samples were examined at University of Nantes, France.

2A. Materials

a. Description & gemological data of samples:

Ref	Image	Color	Shape	TP	Ω-ray	ε-ray	DR	Optic Cha	Pleo	Chelsea Filter	UV LWUV	UV SWUV	SG	Ct. Wt
DSK-1		vstbG	Oval	TP	1.590	1.580	0.010	U	bG-yG	NA	Inert	Inert	2.75	2.84
DSK-2		slyG	Oval	TP	1.587	1.579	0.008	U	yG-bG	NA	wk yellow	Inert	2.75	2.73
DSK-3		vstbG	EC	TP	1.588	1.580	0.008	U	bG-yG	Grey	Inert	Inert	2.74	3.69
DSK-4		vslbG	Oval	TP	1.590	1.580	0.010	U	Weak	Red	Inert	Inert	2.74	2.12
DSK-5		vstbG	Oval	TP	1.590	1.585	0.005	U	bG-yG	NA	Inert	Inert	2.74	2.88
DSK-6		vstbG	Oval	TP	1.590	1.580	0.010	U	bG-yG	NA	Inert	Inert	2.72	2.87
DSK-7		bG	Oval	TP	1.590	1.580	0.010	U	yG-bG	NA	Inert	Inert	2.75	1.06
DSK-8		GB-BG	Oval	TP	1.590	1.580	0.010	U	yG-bG	NA	Inert	Inert	2.75	1.51

Table 2: Ω-ray: refractive index of the ordinary ray, ε-ray: refractive index of the extraordinary ray, DR: birefringence, LWUV: reaction to long wave ultraviolet (365nm), SWUV: reaction to short wave ultraviolet (254nm)

Table 2: Gemological & Physical properties of the samples.

b. Inclusions in samples:

i.   DSK 1

Fig:5 Phlogopite with chlorite like crystal [6]
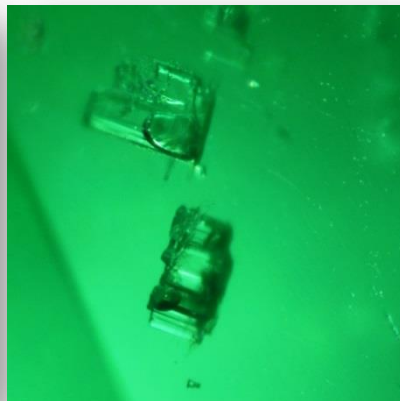
Fig:6 Multiphase rectangular inclusion [12]

Fig: 7 Rectangular multiphase inclusion [12]
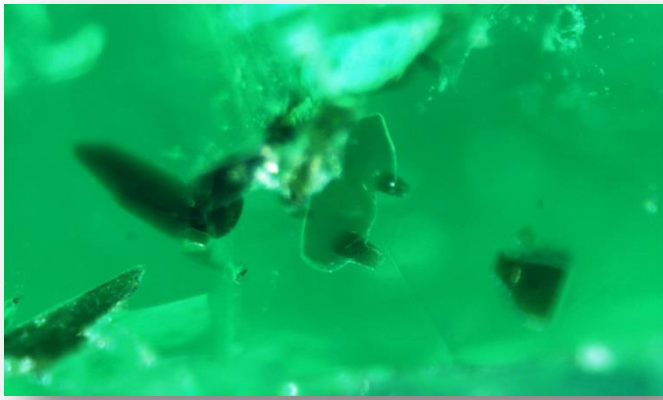
Fig: 8 Platelets of phlogopite [6]
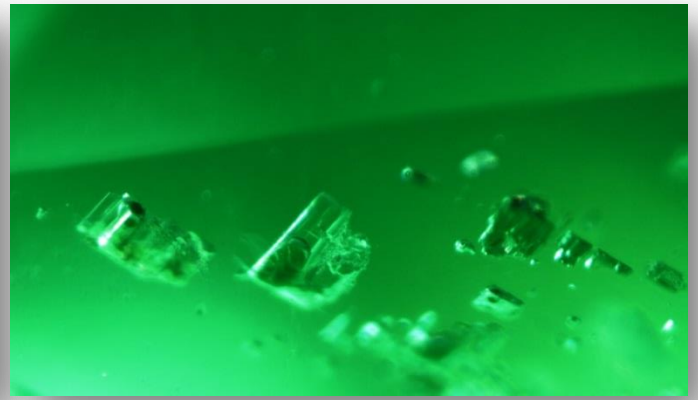
Fig: 9 Rectangular multiphase inclusion [11][6]

DSK 2:
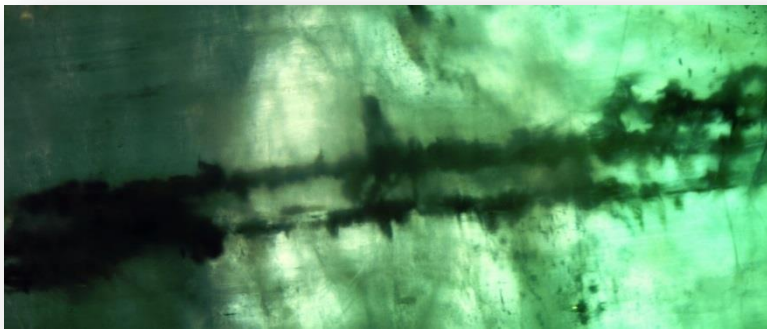
Fig:10 Needle like inclusion probably tourmaline
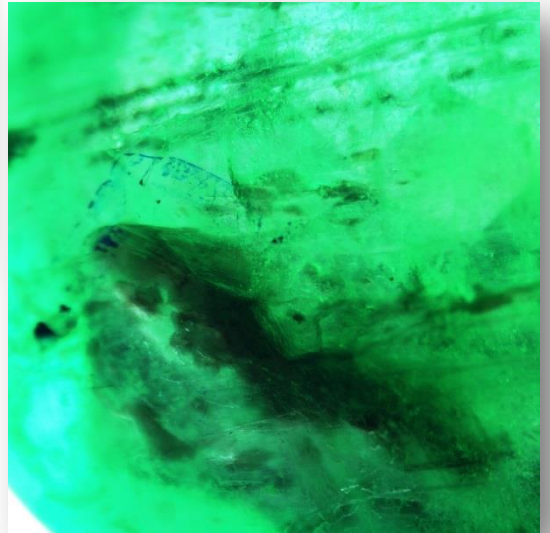
Fig: 11 Phlogopite
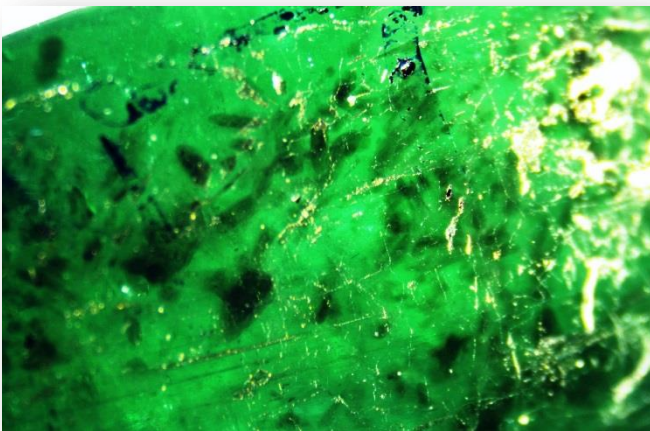
Fig: 12 Platelets of phlogopite [6]

Fig: 13 Needle like inclusions
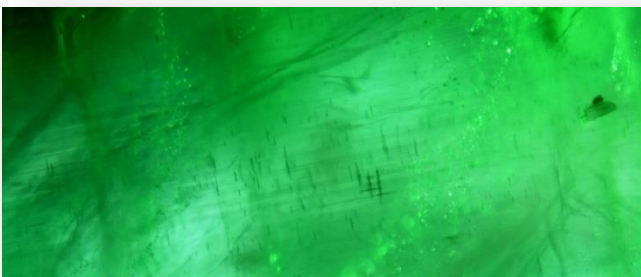
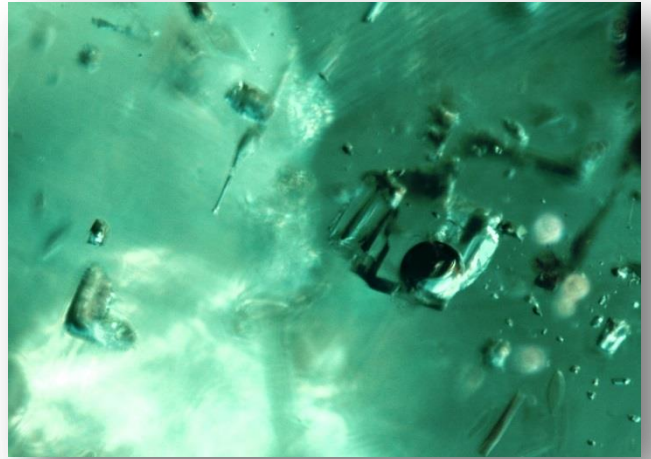*Fig: 14 Needles*

DSK 3:
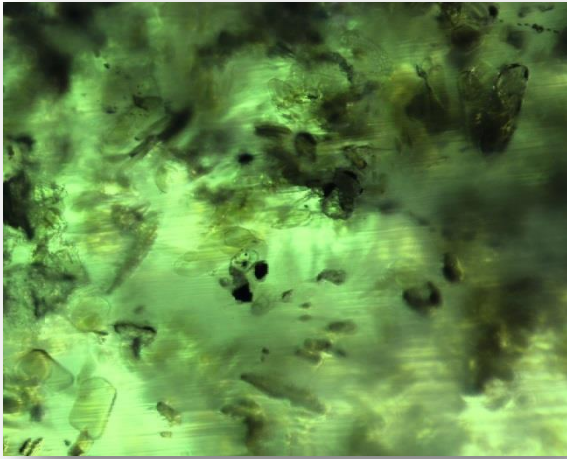
Fig: 15 Platelets of phlogopite [6]

Fig: 16 Irregular multiphase inclusions [12]
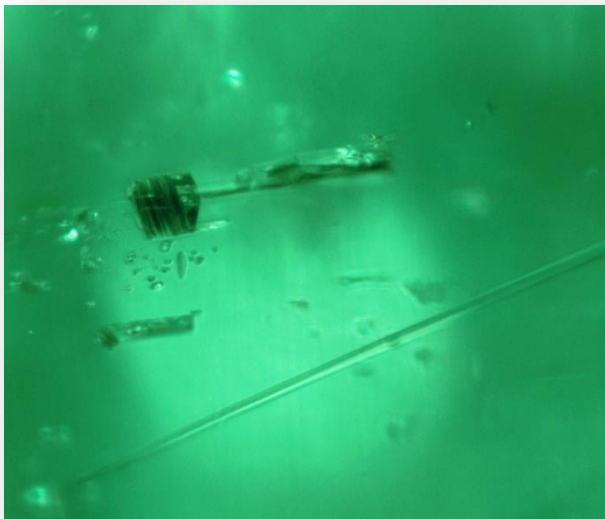
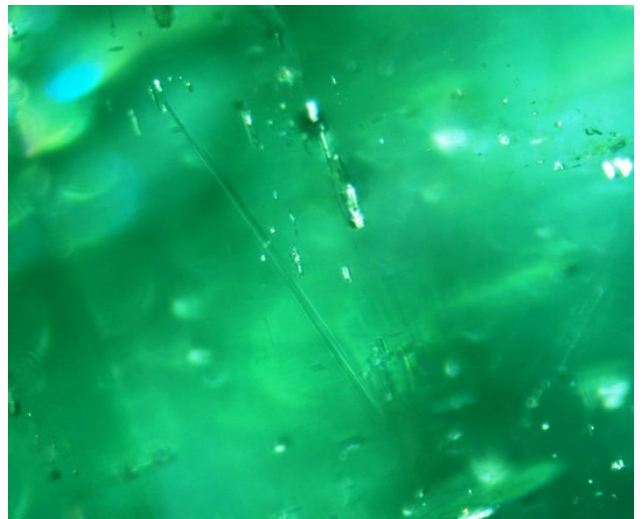*Fig: 17 Colorless needles of actinolite, also seen stacked biotite with multiphase inclusion* [6]

Fig: 18 Colorless needles of actinolite [6]
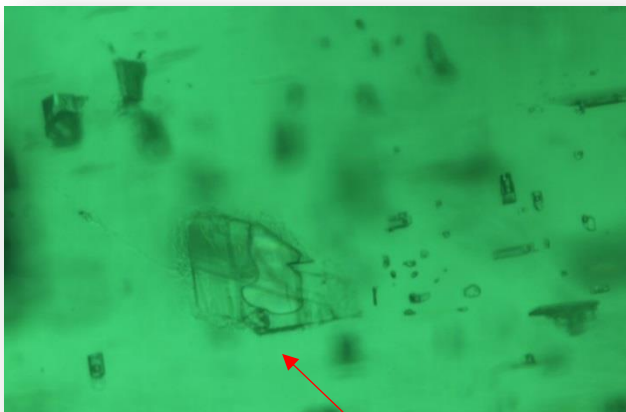
Fig: 19 Irregular multiphase inclusion [6]
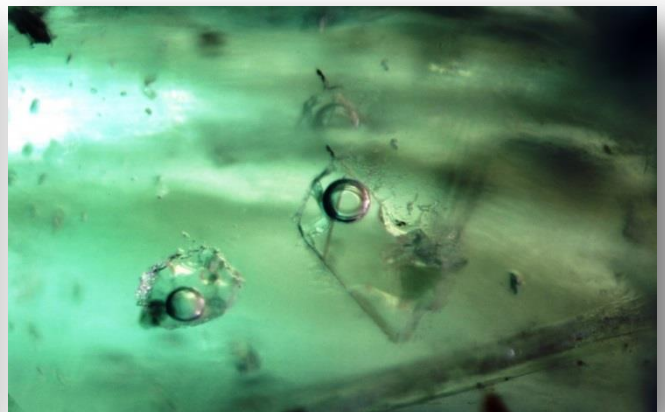
Fig: 20 Irregular multiphase inclusion [6]
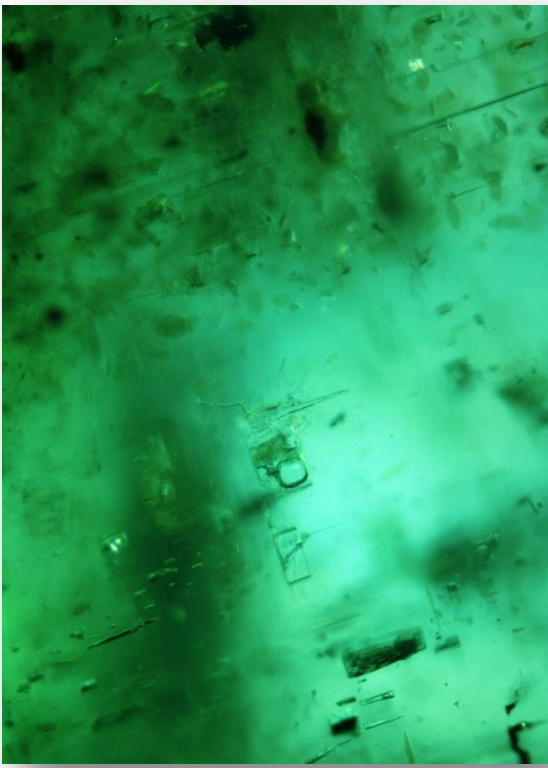
Fig: 21 Irregular multiphase inclusion [6]

Fig: 22 Fluid filled parallel oriented tubes [6]

Fig: 23 Stacking crystals of calcite
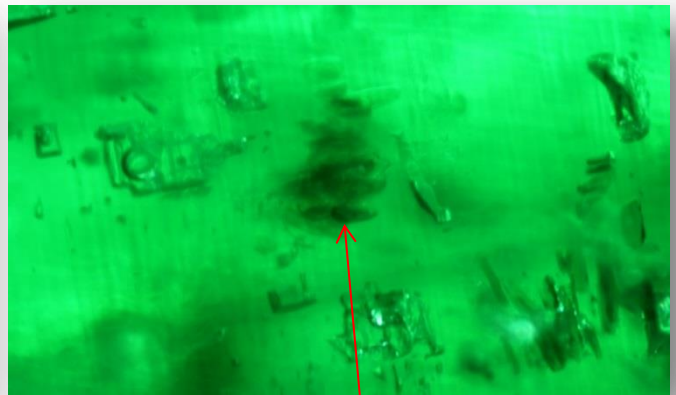
Fig: 24 Irregular multiphase inclusion [6]*, also seen are crystals stacking*
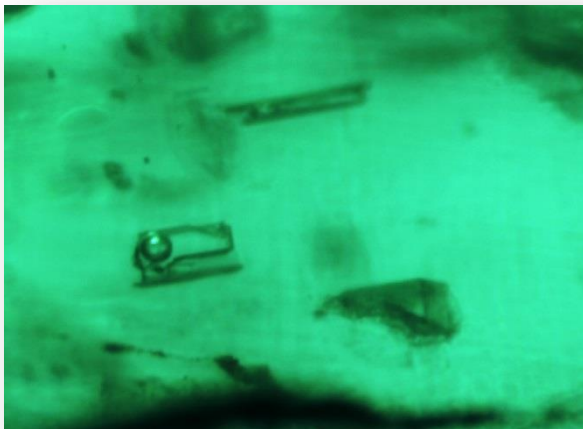
Fig: 25 Rectangular pseudo secondary two-phase inclusion [6]
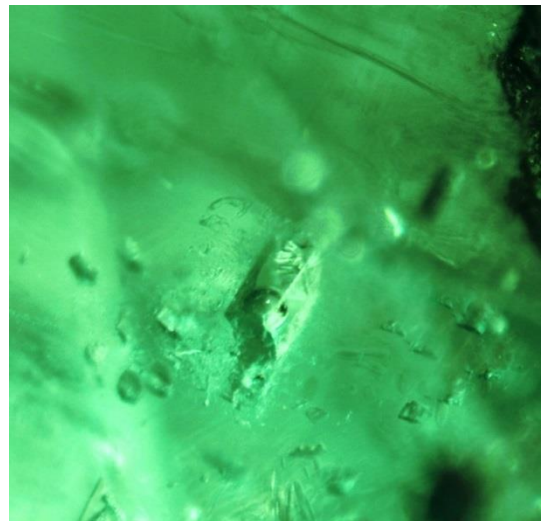
Fig: 26 Rectangular multiphase inclusion [6]

11

DSK 4:
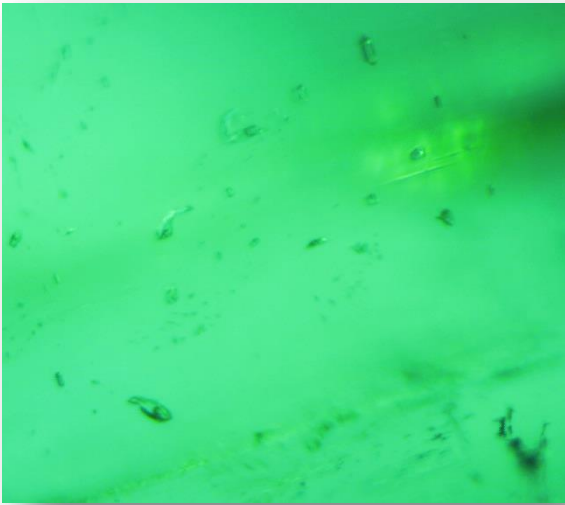
Fig: 27 Multiphase inclusion [6]
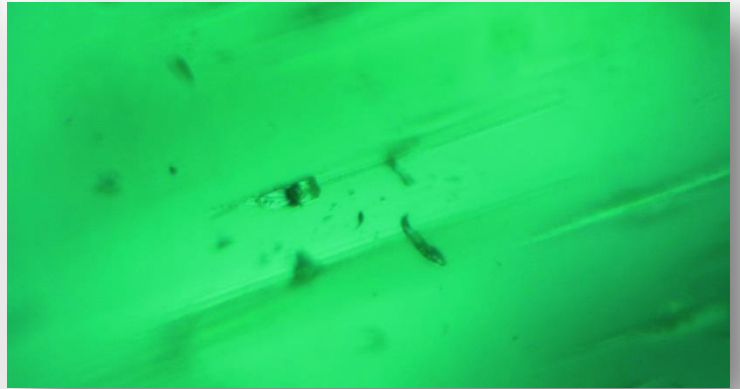
Fig: 28 Multiphase inclusion [6]

DSK 5:

Fig: 29 Phlogopite [6]
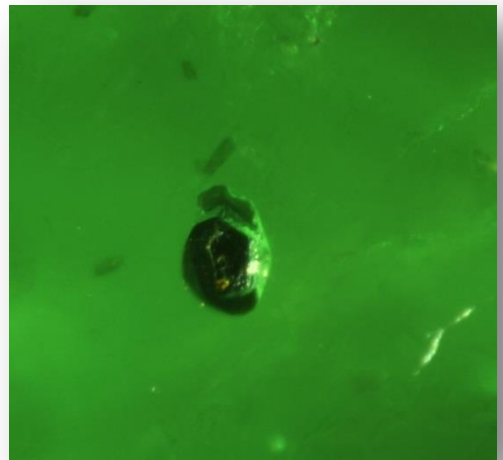
Fig: 30 Metallic opaque crystal of hematite [8]
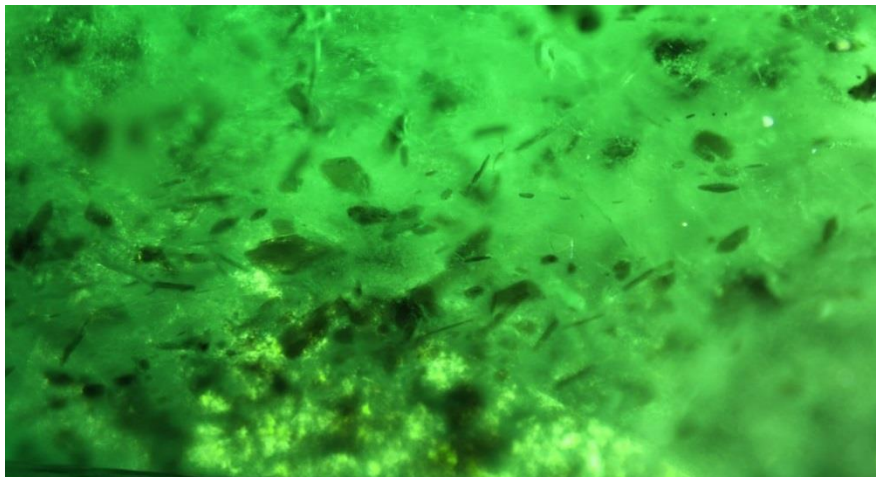
Fig: 31 Platelets of phlogopite in different shapes & sizes [6]

DSK 6:

Fig: 32 Triangular cross sectional view of Tourmaline inclusions [8][9]
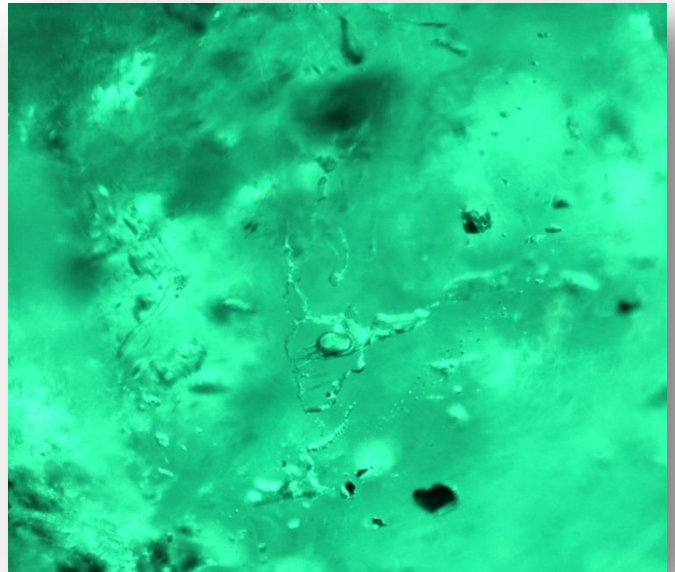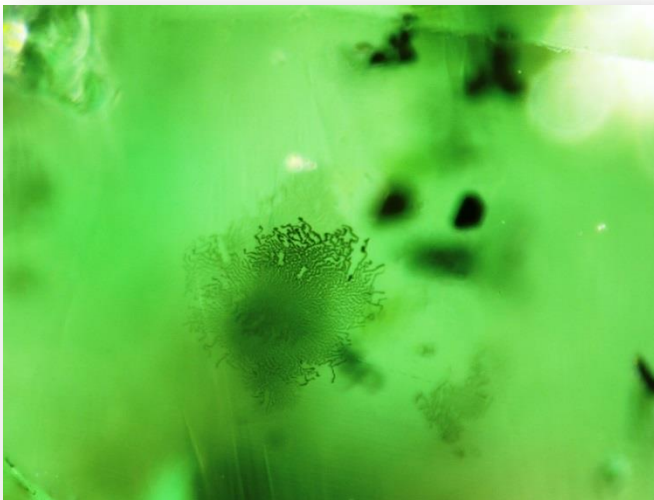

Fig: 33 Three phase along with gas bubble [12]

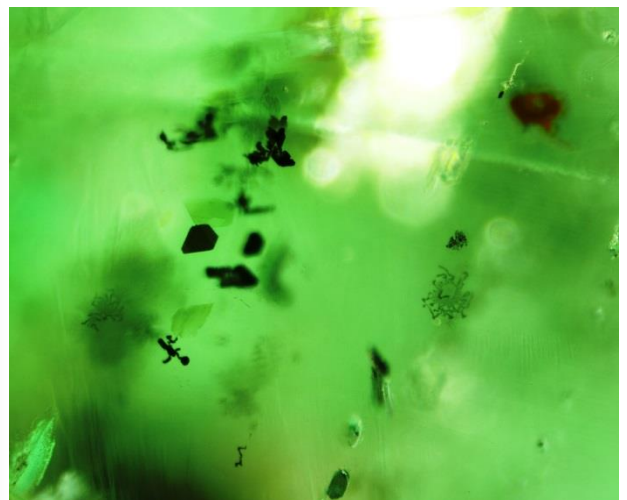*Fig: 34 Dendritic black opaque mineral inclusion probably pyrolusite [12]*

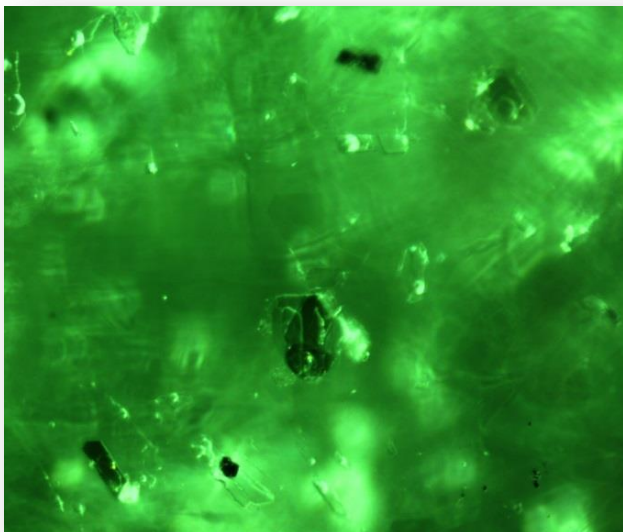*Fig: 35 Dendritic black opaque mineral inclusion probably pyrolusite [12] & hexagonal platelets of hematite*

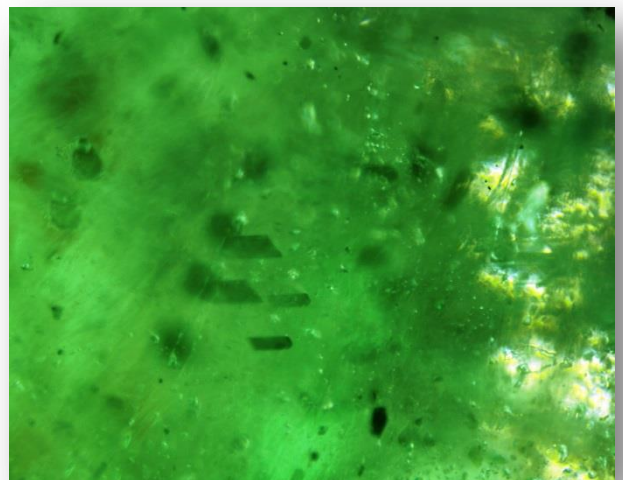*Fig: 36 Irregular multiphase inclusion with biotite platelets [12]*

Fig: 37 Phlogopite/biotite in tube-like appearance

13

DSK 7:

Fig: 38 Phlogopite with actinolite needle at the back [6]

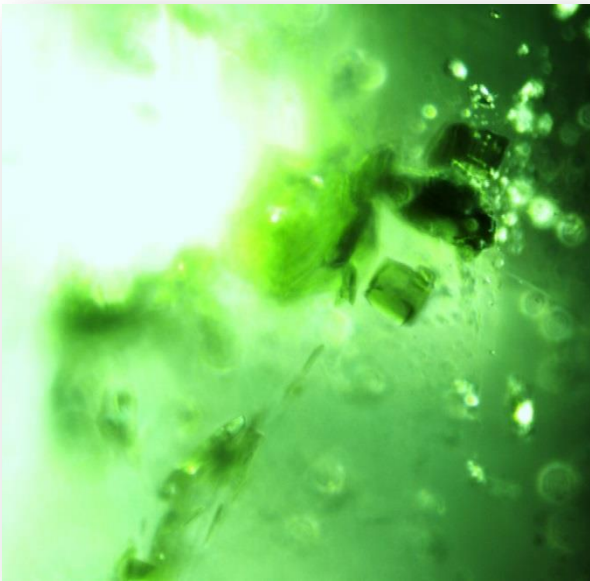*Fig: 39 Platelets of phlogopite in different shapes* [6]

Fig: 40 Platelets of phlogopite in different shapes [6]
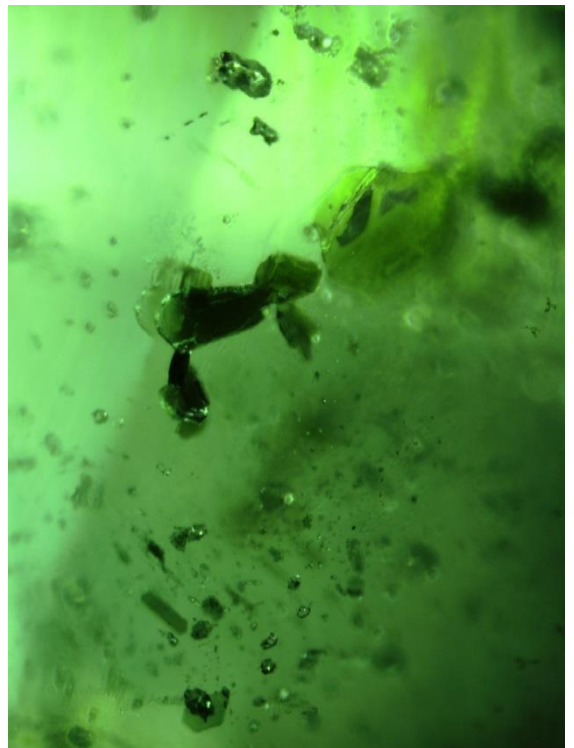

Fig: 41 Platelets of phlogopite in different shapes & multiphase inclusions [6]

DSK 8:

Fig: 42 Irregular multiphase inclusion with bigger crystal of chlorite probably [6]

Fig: 43 Well shaped euhedral Actinolite crystal

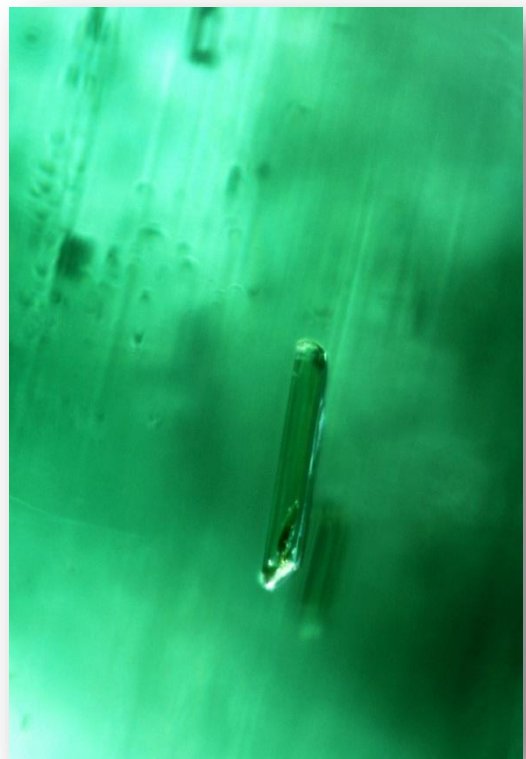**Fig: 44 Well shaped euhedral Actinolite crystal**

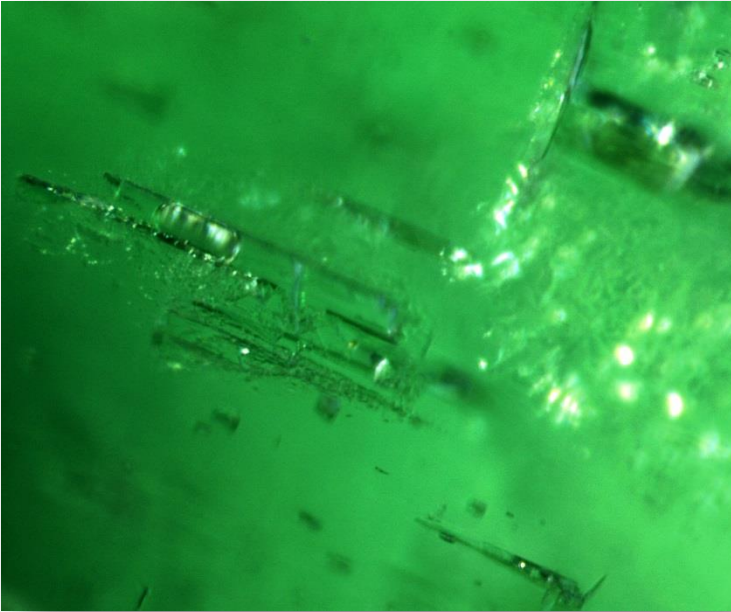**Fig: 45 Well shaped euhedral Actinolite crystal**
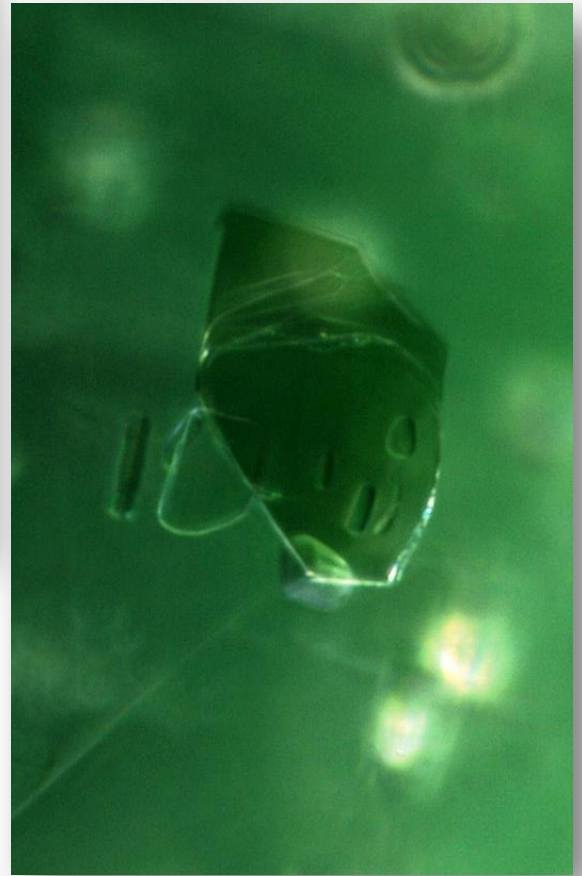
Fig: 46 Rectangular multiphase inclusion [12]

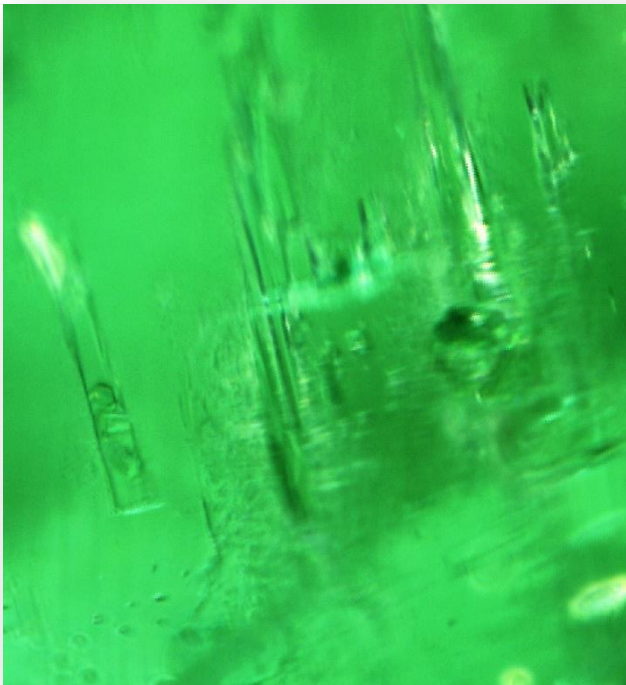*Fig: 47 Platelets of phlogopite* [6]

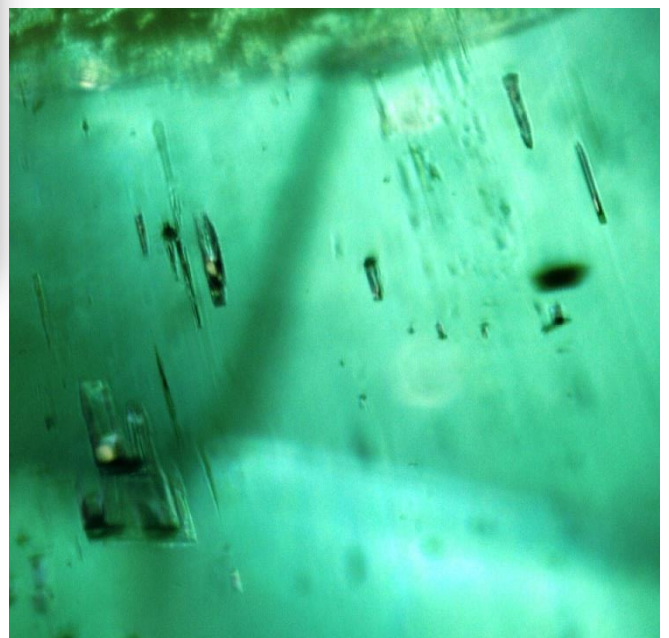*Fig: 48 Rectangular, elongated multiphase inclusions* [12]

Fig: 49 Rectangular, elongated multiphase inclusions [12]

2B. Methods

a. Basic Instruments:

Standard gemological properties were obtained on all the emeralds at GIA campus in Mumbai. I used GIA GEM Instruments Duplex II refractometer with white light and monochromatic light sources to measure the refractive indices and birefringence. Specific gravity was determined using Mettler Toledo by hydrostatic method. Internal features were observed using GIA DLScope Professional Microscope with Leica StereoZoom Magnification from 10x to 64x.

Absorption spectra of the samples were observed using GIA's handheld Diffraction Grating Spectroscope with KRUSS fiber optic light source and prism spectroscope from System Eickhorst Modul 5 spectroscope with built-in light source. Samples were tested for fluorescence using Macbeth Judge-II, in a darkened room under SWUV & LWUV (at IMN-University of Nantes).

b. FTIR:

FTIR was analyzed with BRUKER-ALPHA model (Mid IR 400- 7000^{cm-1}, resolution 4^{cm-1}, number of scans-100).

c. Raman Bruker:

All the samples were also analyzed with Raman (Bruker MultiRAM) using 514nm laser excitation, power 300 mW, resolution 4^{cm-1}, number of scans-100, time–30 seconds.

d. Raman HORIBA T64000:

Inclusions for sample DSK-1, DSK-3 & DSK-6 were analyzed with Raman Microprobe HORIBA T64000 spectroscopy using 514nm laser, number of scans-100, resolution 4^{cm-1}, acquisition- 2 scans each for 30 seconds (at IMN-University of Nantes).

e. Raman LabramHR:

Samples DSK-1, DSK-5 & DSK-7 was analyzed with dispersive Raman spectrometer, LabramHR, 514nm excitation laser at a power of 150 mW, resolution 4^{cm-1}, number of scans-100, time–30/90 seconds. All measurements were conducted using a 50x objective in a confocal configuration to minimize the analysis spot size.

f. Raman STR-300:

Samples DSK-1, DSK-3, DSK-6 & DSK-8 was analyzed with STR-300 (RAMAN), 532 514nm excitation laser at a power of 50 mW, number of scans 10, time 10 seconds, all measurements were conducted using a 20x objective (under the guidance from Mr. Gagan Choudhary from GTL, Jaipur)

g. UV-Vis-NIR:

UV-Vis- Spectrometer analysis for all samples were done using PerkinElmer Lambda 1050 3D WB Detector Module, with conditions- Spectral range 200 to1500 nm, bandwidth at 1 nm, speed 192 nm/min, detector change at 860nm, InGaAs between 0.52 to 10.00s, lamp at 319 nm.

h. SEM:

To study the color and the origin of a gemstone, quantitative chemical analysis of minor and trace elements was performed on samples DSK 1, 2, 3 & 6 using the energy dispersive spectroscopy (EDS) of the scanning electron microscope (SEM). The SEM used is a JEOL JSM-5800LV Scanning Electron Microscope at 20 kV and current of 0.3 nÅ.

i. Nikon Microscope for Inclusions:

Images of inclusions were taken using binocular microscope with Nikon Model P-DF/SMZ18/SHR Plan Apo 1x WD:60/ Digital Sight DS-Ri1, at the GIA India lab in Mumbai (India).

3. Results:

a. Visual Appearance: The colors of most emeralds were ranging from green to slightly bluish green to yellowish green with light to dark tones (**table: 2**). Colors were evenly distributed with not so appealing saturation.

b. Physical Properties:

The refractive indices recorded was fairly constant for most samples with values ranging from n_o = 1.590-1.587 and n_e = 1.579-1585. The birefringence ranged between 0.005-0.010 with one of the stone showing very low birefringence of 0.005. Specific gravity for most stones was 2.74 and 2.75 whilst one of the stone gave an SG of 2.72. (**table: 2**)

While most stones were inert to both long wave and short wave UV, one of the stones showed weak yellow fluorescence. Except two of the stones that appeared gray and red under Chelsea filter, all others were inert. Pleochroism was quite evident in almost all the stones with clear bluish green to yellowish green except one stone that had extremely weak pleochroism. Absorption spectra was seen only in 4 stones ranging between 580-650 nm.

c. Microscopic Characteristics:

Almost all the stones were moderate to heavily included with obvious staining in few, fractures, liquid inclusions and a bunch of biotite.

Fluid inclusions that were elongated, wispy, irregularly shaped often with low relief, many rectangular and tabular shaped were seen that contained either two phases (liquid and gas) or three phases (liquid, gas and solid).

Mineral inclusions such as colorless needles seen were identified by Raman as needles of actinolite. Some of them were straight and few were seen curved. High relief brown to black, elongated, columnar crystals with sharp and rounded triangular cross-section that is typical of tourmaline were also seen in one of the stones. Few phase inclusions were seen associated with crystals.

Three slightly yellowish prismatic and columnar well-formed crystals were seen in one of the samples of different lengths possibly actinolite[6]. Hexagon and irregularly shaped pale to moderate brown biotite/phlogopite were seen that were standing alone and in groups or bunches, relating to their mica schist-metabasite rock formation.

Few stones showed red-orange staining probably due to presence of hematite [5] and dendritic like black opaque inclusion (probably pyrolusite) was also seen[12]. A euhedral spicule shaped like inclusion with a conical base had calcite at the head, limonite in the center and goethite at the conical end identified by Raman peak at 1320^{cm-1}.

d. FTIR (Fourier Transform Infra-Red

The spectrums in ***fig: 51-54*** shows peak at 5263^{cm-1}, 5281^{cm-1}, 5293^{cm-1}, 5281^{cm-1} respectively that are caused by the vibration of water molecules adjacent to alkali-metal ions in the channels of the beryl structure. The broad band between 3800^{cm-1} and 3400^{cm-1} observed in all the spectrums is caused by water molecules in the position, and by free water molecules.[6]

e. Raman (Bruker MultiRAM)

The Raman analysis in ***fig: 55-62*** shows peaks between 321^{cm-1}-326^{cm-1} which is related to ring vibration of emerald, the peaks between 325-395^{cm-1} relates to the deformation mode of the tetrahedral ring, the peak at around 687^{cm-1} – signature of ring stretching of Be-O bond and peak at around 1066^{cm-1} is attributed to Be-O stretching and Si-O stretching of vibration beryl crystal.[10]

f. Raman Microprobe HORIBA T64000

Raman bands observed in ***fig: 63-71*** at around 324^{cm-1}, 392^{cm-1}, 445^{cm-1}, 525^{cm-1}, 622^{cm-1}, 673^{cm-1}, 1080^{cm-1} are typical emerald bands and peak at 324^{cm-1} matches the beryl Si_6O_{18} ring breathing mode, additional Raman-active modes near 750^{cm-1} (Al) and above 855^{cm-1} (Be), this is due to significant mixing of Al and Be motions with those of the ring. [10]

Different peaks like 290^{cm-1} indicates presence of Hematite, 432^{cm-1} (OH-Stretching), 557^{cm-1} (Deformation of Si_4O_{11}), 664^{cm-1} (Magnetite), 679^{cm-1} (Si-O-Si Stretching), 968^{cm-1} (Absorption of O-Si-O) and 1007^{cm-1} (Zircon) belongs to Type-I (without alkali nearby). [10]

The peaks at around 284^{cm-1}, 715^{cm-1} and 1080^{cm-1} respectively indicates the presence of singly refractive solid (cubic) crystals consisting of halides, daughter crystal identified as calcite. [10]

Fig 68 shows peaks around 3567^{cm-1} relating to water type-II (water molecules with alkali ions nearby) and peaks around 3609^{cm-1} indicates water type-I (those water molecules without any presence of alkali ion nearby), as explained by Reshma B et al. [11]

g. Raman spectrometer, LabramHR

Observations matched to peaks seen in Raman HORIBA T64000. (*fig: 72-79*)

h. RAMAN STR-300 (GTL, Jaipur)

DSK-1

Some of the most common inclusions found in Zambian emeralds were observed like phlogopite (mica-biotite as subhedral to anhedral ultra-thin transparent platelets or thicker translucent to nearly opaque), the color of the mica-biotite was reddish-brown to greyish-brown. Multiphase inclusion hosting a dolomite (brown color) crystal represented by peaks around 1091^{cm-1} was observed. Peak at 1625^{cm-1} and 1385^{cm-1} vaguely indicates presence of fluid and gas. Most crystals were associated with phase inclusions either multiphase or two-phase. (*fig: 80-85*) [3][6][8] [12]

DSK-3

A spicule shaped inclusion with calcite towards the head, followed by limonite in the center and the conical shape ending with goethite was seen with peaks around 190^{cm-1} (mica), calcite, limonite/goethite around $1320^{cm-1.}$ Some fibrous needle like inclusions were observed with peaks at 673^{cm-1} indicating presence of actinolite. Stacking crystals of calcite in a step-like pattern overlapping with aragonite peaks at 1085^{cm-1} was observed. Brown patches/staining indicated stains from hematite, limonite or polishing compounds. (*fig: 86-90*) [3][6][8] [12]

DSK-6

A black to dark brown color tube-like columnar crystal was seen with typical trigonal outline and sharp peak at 221^{cm-1} indicating presence of tourmaline. Tourmalines are found throughout the schist host rock in direct association with the emeralds and thus it is not surprising to find tourmaline crystals as inclusions in the emeralds from Zambia. Also observed were some red-orange color platelets-few having hexagonal outline and many other had random shapes, some were dendritic-fern shaped showing typical peaks of Hematite at 1320^{cm-1}. (*fig: 91-92*) [3][6][8] [12]

DSK-8

Elongated, prismatic rod shaped transparent crystalline inclusions with peaks at 1091^{cm-1} indicating actinolite. Some of the actinolite were acicular, curved and straight. Short crystals and traces of Hematite (1320^{cm-1}) were observed. Most of the samples showed rectangular/cubic multi-phase inclusions intersecting at times with phlogopite (biotite) platelets. (*fig: 93-95*) [3][6][8] [12]

i. UV-Vis-Spectrometer

Emeralds from Musakashi (Zambia) shows lower V^{3+} and no Fe^{2+} related bands at around 810nm or Fe^{3+} bands at around 372nm whereas emeralds from Kafubu (Zambia) shows strong absorption of Fe^{3+} with bands around 373nm and 810nm absorption related to Fe^{2+}.[12]

Absorption band at around 427nm indicates emeralds colored by Cr^{3+} ions that are located in octahedral Al^{3+} sites.[5] Most common peaks observed in almost the samples were at around 860nm relating to Fe^{2+} [1] and peaks for Cr^{3+} at around 425^{cm-1}, 610^{cm-1}, 662^{cm-1}, 684^{cm-1} were seen in 5 samples out of the 8 samples that were tested (*fig:96-105*).

The higher concentrations of Fe^{2+} may lead to indicate Kafubu (Zambia) origin although UV-Vis spectra can only distinguish origin to a limited extent.[6] It is also obvious that there was some experimental errors due to which few of the results obtained were not very accurate.
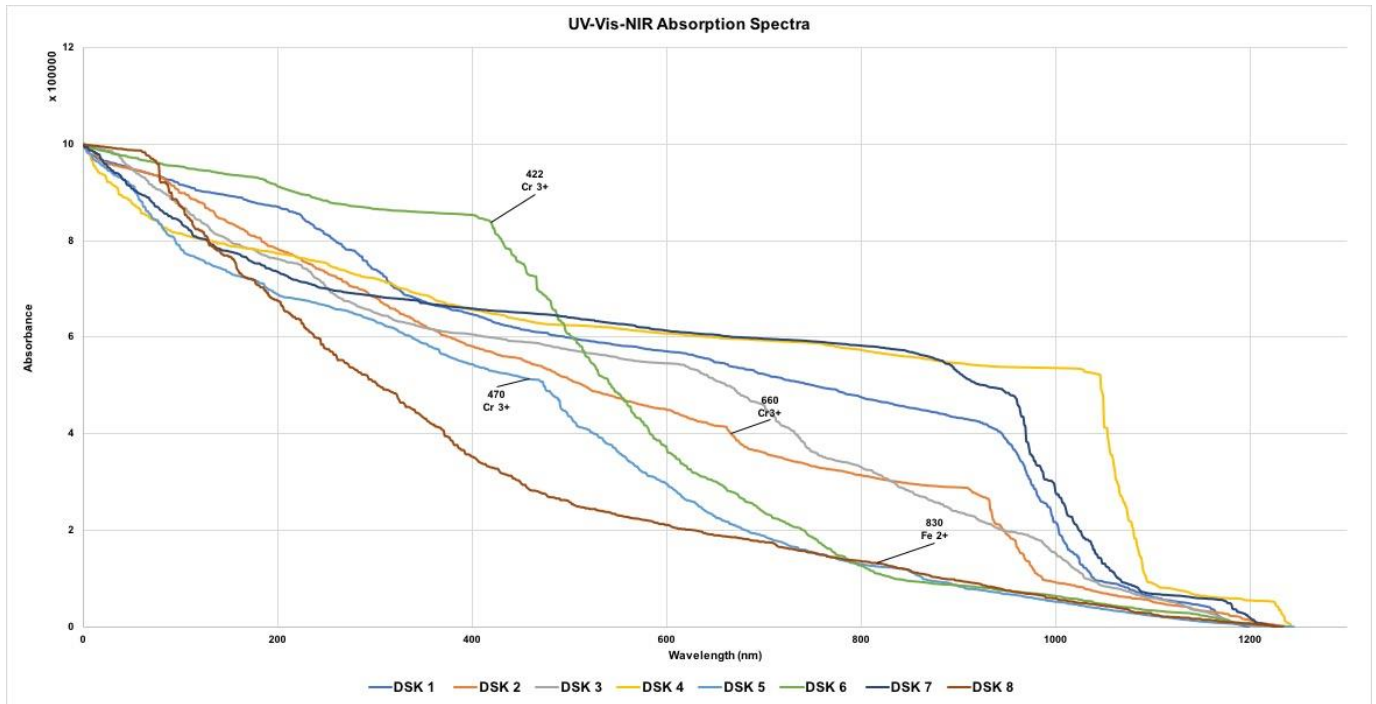
Fig: 50 UV-Vis-Spectra comparison between all samples

j. SEM (Scanning Electron Microscope)

According to studies done by Zwaan et al. (2005) they mention some amount of chromium (Cr) content in Zambian emeralds anywhere from 0.26% to 0.86 % and sometimes as low as 0.04 % which can be observed in sample DSK-2. The other samples did not show significant amount of chromium for any analysis. They also mention 0.02 % of vanadium (V) seen in emeralds from Zambia but in my samples I could not find any traces of vanadium.

Traces of iron (Fe) from 0.76% to 1.75%, magnesium (Mg) and sodium (Na) at around 1.90% & 1.10% respectively which could be seen in some of my samples DSK 1,2,3 & 6. (*table 3*).[6] Lighter elements like beryllium could not be detected due to limitations posed by the instrument itself as mentioned during instrument demonstration by B. Rondeau.[6]

Element → Samples ↓	O	Na	Mg	Al	Si	K	Cr	Ca	Fe	AT%
DSK-1	63.95	1.64	1.45	6.91	26.03	0.00	0.00	0.00	0.00	100
DSK-1	68.74	1.62	1.52	6.09	21.99	0.00	0.00	0.00	0.00	100
DSK-1	57.78	0.29	12.61	6.03	17.10	4.04	0.02	0.00	2.13	100
DSK-2	66.18	1.29	0.84	6.98	24.54	0.04	0.03	0.00	0.10	100
DSK-2	57.02	0.40	12.50	6.02	17.47	4.41	0.04	0.00	2.14	100
DSK-3	50.66	0.04	14.04	5.95	20.70	5.88	0.00	0.02	2.71	100
DSK-6	60.68	1.68	5.36	14.93	15.64	0.00	0.00	0.26	1.46	100
DSK-6	60.86	1.72	5.29	14.82	15.63	0.00	0.00	0.25	1.44	100

Table: 3 - SEM Analysis Report

4. Discussion

a. Physical Properties:

The refractive indices (n_o = 1.590 and n_e = 1.579), birefringence of 0.005-0.010 and specific gravity 2.72-2.75 were nearly consistent with those presented by Zwaan et al. (2005) and Saeseaw et al. (2014). The pleochroic colors seen with dichroscope were yG and bG. (**table: 2**) [6]

b. Chemical Properties:

Chemical analyses showed a wider range of trace-element concentrations but the Cr content was fairly low to what has been reported by Zwaan et al. (2005); however, a wider range of Mg, Al and Si concentrations was seen compared to Na, Ca and K with no traces of V. It was interesting to note as reported that the Zambian stones generally show a low V content, a moderate amount of Cr, Mg, and Na, and a moderate-to-high Fe content, which supports our analysis. (**table:1 & 3**)[6]

c. Inclusions:

Inclusions in Zambian Emeralds have been described by Koivula (1984), Graziani et al. (1984), Moroz et al (1996), Moroz et al. (1999), Antonín et al. (2004), Zwaan et al. (2005) and Saeseaw et al. (2014) and many of the inclusions described- support as seen in the samples. However, inclusions like glauconite, chrysoberyl, margarite, muscovite, or chrysotile were not present as described by Graziani et al. (1983), which suggests that these mineral inclusions are rare. Many isolated CO_2-CH_4 bearing negative crystals were seen as reported by Zwaan et al. (2005).[6] (**table: 4**)

The most common inclusions seen were phase inclusions, containing colorless transparent crystals and a gas bubble suspended in a fluid (fig: 6,7,9,16,19,20,21,22,25,26). Such inclusions were seen in almost all the samples. Some multiphase inclusions also hosted one or more small dark to black crystals, and occasionally tiny colorless or whitish crystals, some of these inclusions were identified by Raman spectroscopy. The gas phase was identified as CO_2 (peaks at 1284[cm-1] and 1387[cm-1]). The crystals displayed only the emerald spectrum and no Raman lines, suggesting they could be halides.[2]

Daughter crystals were identified as calcite (peaks at 283, 713, and 1085^{cm-1}), brownish crystals as dolomite (peak at 1091^{cm-1}). Some tubular tourmaline inclusions were observed with peaks at 221^{cm-1}. [1][3][6][8] [10] [12]

Whilst there are only a few who have mentioned about presence of dolomite crystal in Zambian emeralds which is due to the schist-type rocks Zambian emeralds form in, one such dolomite crystal associated with phase inclusion was observed in sample DSK 1 and this was identified by Raman peak at 1091^{cm-1} (as mentioned earlier). [1][4] [10]

Similar inclusions have been found in Colombian emeralds (Giuliani et al., 1994). The shape of the multiphase inclusions was usually irregular, some fern like branches were also observed. In few needle-like inclusions of actinolite was also observed. Under darkfield illumination, tube-like growth features resembling tourmalines were seen with triangular cross-section.

Earlier research on emeralds have reported that Emeralds from Zambia are commonly associated with quartz, pyrite, dark brown to black tourmaline, mica, and chlorite and thus these dark, opaque inclusions were identified by Raman spectroscopy as tourmaline. [3] [8][9]

Of the 8 emeralds, only one (DSK-8) showed mineral inclusion that was colorless to pale yellowish and transparent euhedral and not part of multiphase inclusions which was identified using Raman spectroscopy (peak at 673^{cm-1}) as actinolite crystals. Also found were several opaque and metallic inclusions resembling iron oxide, possibly hematite/goethite.

The multiphase inclusion seen had different geometric shapes with quite irregular outline. Most of these hosted some liquid and a gas bubble, but in few a solid third phase was also seen. The crystal associated had very low relief. *Fig: 5-49 (images of all inclusions)*

d. FTIR:

Out of the 8 stones, 4 stones tested with FTIR shoed peaks around 5265^{cm-1}, that are caused by type II H_2O molecules, which are present in the channels of the crystal structure of beryl. As explained by Zwaan et al. (2005) these water molecules are located adjacent to alkali-metal ions in the channels which in the Zambian emeralds are mainly Na^+, Cs^+, and Li^+. Zwaan et al. (2005) further explains that the broad band roughly between 3900^{cm-1} and 3400^{cm-1} is caused by type I and type II H_2O molecules and the peak at 2359^{cm-1} is caused by CO_2, this peak was seen in only one of the sample for which spectra were taken.[6]

The peaks at around 2930^{cm-1} is probably due to fillers used for clarity enhancement (Choudhary 2017, Zwaan et al. 2005), although no yellow or blue flash effects were observed (a possible indication that an artificial resin might be present) in the fissures. [2][6]

e. UV-Vis-NIR:

Strong Fe^{2+} absorptions with lower Cr^{3+} were observed in almost all the stones. Between Kafubu & Musakashi emeralds, the latter has strong absorption to Fe^{2+} but similar absorptions have been reported in emeralds from Panjshir, Afghanistan. It thus indicates that UV-Vis spectra's only help distinguish between certain emerald origins to a limited extent which is indicated by differences in the valence state of iron. (*table:5*) [12]

Properties		Kafubu area, Zambia	Santa Terezinha de Goias, Brazil	Itabira district, Brazil	Ural Mountains, Russia	Mananjary region, Madagascar	Sandwana, Zimbabwe	Swat Valley, Pakistan	Habachtal, Austria
Physical and optical properties									
References		This study, Milisenda et al. (1999)	Lind et al. (1986), Schwarz (1990a; 2001)	Hänni et al. (1987), Schwarz et al. (1988), Epstein (1989); Henn and Bank (1991); Gübelin (1989), Schwarz (1998), Zwaan (2001)	Gübelin (1974), Sinkankas (1981), Bank (1982), Mumme (1982), Schmetzer et al. (1991), Gübelin and Koivula (1986), Laskovenkov and Zhernakov (1995)	Hänni and Klein (1982), Schwarz and Henn(1992), Schwarz (1994)	Gübelin (1958), Zwaan et al. (1997)	Henn (1988), Gübelin (1989)	Gübelin (1956), Morteani and Grundmann (1977), Nwe and Grundmann (1990), Schwarz (1991), Gübelin and Koivula (1986), Grundmann (2001)
RI									
	n_0	1.585-1.599	1.592-1.600	1.580-1.590	1.581-1.591	1.588-1.591	1.590-1.594	1.584-1.1600	1.582-1.597
	n_e	1.578-1.591	1.584-1.593	1.574-1.583	1.575-1.584	1.580-1.585	1.584-1.587	1.578-1.591	1.574-1.590
Birefringence		0.006-0.009	0.006-0.010	0.004-0.009	0.007	0.006-0.009	0.006-0.007	0.006-0.009	0.005-0.007
S.G.		2.69-2.78	2.75-2.77	2.72-2.74	2.72-2.75	2.68-2.73	2.74-2.77	2.70-2.78	2.70-2.77
Distinguishing internal features		Skeletal magnetite and hematite (if present)	Abundant opaque inclusions, such as black spinel octahedrons; pale brown to colorless carbonate rhombohedra; fluid inclusions are very small and rare	Numerous parallel growth tubes (with remarkable variation of fluid inclusions)	Irregular color distribution (if present)	Elongate quartz crystals, parallel to the c axis, growth tubes; fibrous aggregates of talc (if present); rhombohedral carbonate crystals (rare)	Abundant thin needles and curved fibers of amphibole; extremely small fluid inclusions (if present); black grains of chromian ilmenorutile (very rare); phlogopite virtually absent	Many two-and three-phase inclusions (similar to Colombia), but with no rectangular to square shapes; common black chromite and rhombohedral dolomite	Commonly show patchy color distribution; most stones are heavily included and fractured (rarely cut table and only in small sizes)
Iron peaks in UV-VIS spectra		Fe^{2+} and Fe^{3+} features	Fe^{2+} and Fe^{3+} features	Fe^{2+} and Fe^{3+} features	Fe^{2+} features only, or Fe^{2+} and Fe^{3+} features	Fe^{2+} and Fe^{3+} features	Fe^{2+} features only	Fe^{2+} and Fe^{3+} features	Fe^{2+} and Fe^{3+} features

Table:4 - Properties of emeralds with R.I. and S.G. values similar to those from Kafubu, Zambia [6]

5. Conclusion

Jagged three phase inclusions for many years was a key indicator of Columbian Emeralds but emeralds that are seen currently in the market also display similar jagged three phase inclusions making origin determination a challenge. These emeralds were reported to be from Panjshir (Afghanistan), Davdar (China), and Kafubu and Musakashi (Zambia) (Saeseaw et al. 2014).[12]

Musakashi (Zambia) emeralds are dominated by multiphase inclusions that are irregular with no particular shape or outline than those more commonly seen in Colombian emeralds. These multiphase inclusions from Musakashi (Zambia) have one or two crystals associated with gas bubble similar to Colombian origin. Similar multiphase inclusions are also reported in emeralds from Davdar, China.[12]

Emeralds that form in localities belonging to schist-type usually contains inclusions of mica, chlorite, calcite, dolomite, apatite, quartz, pyrite, plagioclase and these localities include Australia, Brazil, Mozambique, Russia, Tanzania and Zambia.[1][4]

Thus study of inclusions alone cannot identify origin of emeralds, combination of tests such as spectroscopy and trace element chemistry may provide valuable information to distinguish origin. The difference between the Fe^{2+} or Fe^{3+} or the intensity of V^{3+} absorption may help in suggesting origin.[12]

Locality	Refractive Index	Color Filter Reaction	Microscopic Characteristics	UV-Vis Spectroscopy (Cations in addition to Cr3+)	Trace-element analysis
Musakashi, Zambia	1.572–1.582	Strong pink	Multiphase inclusions tend to be more irregular than those in Colombian gems; multiphase inclusions with at least two crystals associated with a gas bubble may indicate Zambian rather than Colombian origin	No significant Fe2+-related absorption features in the NIR region, and no Fe3+ observed	Low alkali metal concentrations (1,530–6,060 ppmw) Cr > V; Cr/V ratio 1.7–5.3 Fe concentration: 680–1,490 ppmw Li vs. Cs log-log plot can help separate Musakashi from Kafubu and slightly separate from Colombia Fe vs. K log-log plot can help separate Musakashi from Colombia
Kafubu, Zambia	1.582–1.593 (RI values typically higher than other localities)	Inert	Multiphase inclusions are usually rectangular in shape, but may be irregular in outline; solid crystals of pyrolusite, chlorite, mica, amphibole, and tourmaline	Strong broad Fe2+ band at approximately 810 nm O-ray: narrow Fe3+ band at approximately 372 nm	High alkali metal concentrations (15,834–23,294 ppmw) Cr >> V; Cr/V ratio 8–40 Fe concentration: 5,900–11,600 ppmw Li vs. Cs log-log plot can help separate Kafubu from others
Panjshir Valley, Afghanistan	1.572–1.590	Inert to pink	Multiphase inclusions tend to be more elongated or needle shaped than other localities; each may host several cubic to rounded transparent crystals, and sometimes small, dark opaque crystals	Medium broad Fe2+ band at approximately 810 nm O-ray: Fe3+ peak at 372 nm in some samples	Moderate to high alkali metal concentrations (3,946–17,505 ppmw) Cr and V concentrations may be similar: Cr/V ratio 0.3–3.3 Fe concentration: 1,010–9,820 ppmw Li vs. Cs log-log plot can help separate Panjshir from Kafubu, Musakashi, and Colombia (and Davdar, to a lesser extent)
Davdar, China	1.577–1.588	Pink	Multiphase inclusions are usually jagged or irregular in outline, and some are needle-like	Similar to Musakashi: Small broad Fe2+ band at approximately 810 nm Similar to Colombia: Strong V3+ bands at approximately 400 and 654 nm	Low to moderate alkali metal concentrations (5,190–12,620 ppmw) Slightly more V than Cr; Cr/V ratio 0.1–1.0 Fe concentration: 1,230–4,350 ppmw Fe vs. K log-log plot can help separate Davdar from Musakashi and Colombia Li vs. Cs log-log plot can help separate Davdar from Panjshir, to a lesser extent
Colombia (Muzo, Coscuez, La Pita, Peñas Blancas, and Chivor)	1.570–1.580 (typically lower than other localities)	Pink to strong pink	Classic jagged multiphase inclusions host a gas bubble and one or more cubic crystals; gas bubbles are usually smaller than the whole inclusion, and also smaller or about the same size as the associated cubic crystal	No Fe2+ or Fe3+ observed Weak to medium V3+ bands at approximately 400 and 654 nm	Low alkali metal concentrations (1,515–8,115 ppmw) Cr and V concentrations may be similar: Cr/V ratio 0.04 and 3.5 Fe concentration: 117–2,030 ppmw Fe vs. Ga and Fe vs. K log-log plot can help separate Colombia from others

Table: 5 Summary of physical properties, UV-Vis-NIR absorption data, and trace-element chemistry of emeralds from five different localities. [12]

6. Acknowledgement

After an intensive period of 5 months, writing this note of thanks is the finishing touch on my dissertation. It has been a period of intense learning for me, not only in the scientific arena, but also at a personal level. Writing this dissertation has had a big impact on me. I would like to reflect on all those people who have supported guided and helped me so much throughout this period.

I would first like to thank Mr. Gagan Choudhary, who supported me greatly and was always willing to help me. He not only gave me access to Gem Testing Laboratory (GTL) Jaipur, India but also shared his immense knowledge and valuable time which enabled me to carry out the final tests necessary to create this report.

I would also want to thank Mr. Dheeraj Gupta from GJSPC Laboratory Delhi, India, who was very kind to donate the samples for my experimental project.

In addition, I would like to thank my professors Dr. Emmanuel Fritsch and Dr. Benjamin Rondeau for their valuable guidance, excellent cooperation and for all of the opportunities given to conduct my research and further my dissertation. They definitely provided me with the tools that I needed to choose the right direction and successfully complete my dissertation.

7. References

1. A. V. Seifert, V. Žáček, S. Vrána, V. Pecina, J. Zachariáš, J. C. (Hanco) Zwaan – "*Emerald mineralization in the Kafubu area, Zambia*" - Bulletin of Geosciences, Vol. 79, No. 1, 1–40, 2004 - © Czech Geological Survey, ISSN 1214-1119.

2. G. Choudhary – "Identifying fracture filling in emerald: - JAS 2017

3. G. Graziani, E. Gubelin, S. Lucchesi - "*Report on the investigation of an Emerald from the Kitwe District, Zambia*" – The Australian Gemmologist, Volume 15, Number 7, August 1984.

4. I.I. Moroz and I.Z. Eliezri – *"Mineral inclusions in Emeralds from different sources*" – The Journal of Gemmology, Vol 26. No. 6, April 1999.

5. I. I Moroz, Michael L.Roth, Valery B.Deich – "*The Visible Absorption Spectroscopy of Emerald From Different Deposit*s". Australian Gemmologist (1999) 20,315-320, page 316.

6. J. C. (Hanco) Zwaan, Antonín V. Seifert, Stanislav Vrána, BrendanM. Laurs, Björn Anckar,William B. (Skip) Simmons, Alexander U. Falster,Wim J. Lustenhouwer, SamMuhlmeister, John I. Koivula, and Héja Garcia-Guillerminet – "*Emeralds From The Kafubu Area, Zambia*" - *G&G, Summer-2005*

7. J. C. (Hanco) Zwaan, Dorrit E. Jacob, Tobias Häger, Mário T. O. Cavalcanti Neto, and Jan Kanis- "*Emeralds from The Fazenda Bonfim Region, Riogrande Donorte, Brazil*" – *G&G, Spring 2012* - page 10-11.

8. J. Koivula – "*Mineral inclusions in Zambian Emeralds*" - The Australian Gemmologist, Volume 15, Number 7, August 1984.

9. J. Koivula – "*Tourmaline as an inclusion in Zambian Emeralds" – G&G, Winter 1982*

10. Jena PR and Mishra PK - "*Microstructural, Raman, EPMA and X-ray Tomographic Study of the Odisha's Beryl (Emerald) Sample*"- Journal of Geology & Geophysics- 2017, Volume 6 • Issue 3 • 1000288-ISSN: 2381-8719 – page 2-3.

11. Reshma B, Sakthivel R and Mohanty JK- "*Characterization of Low Grade Natural Emerald Gemstone"* - Journal of Geology & Geophysics- Vol 6-Issue 1- ISSN-2381-8719 page 4.

12. S. Saeseaw, V. Pardieu, S. Sangsawong- "*Three-phase inclusions in Emerald and their impact on origin determination"*- G&G, Summer-2014

13. https://en.wikipedia.org/wiki/Emerald.

14. https://collectorsedge.com/pages/the-kagem-emerald-mine-kafubu-area-Zambia.

15. https://www.gemrockauctions.com/learn/additional-gemstone-information/zambian-emeralds-what-you-need-to-know

8. Annexures:

FTIR (Fourier Transform Infra-Red)

DSK-1 Fig 51
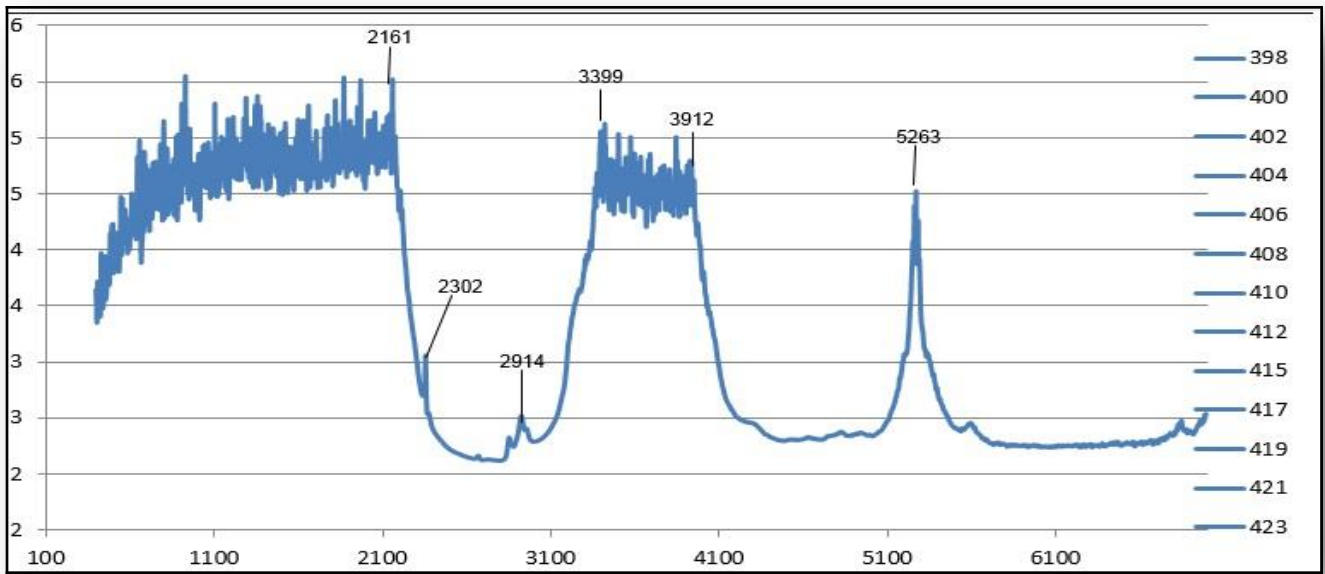
DSK-4 Fig 52
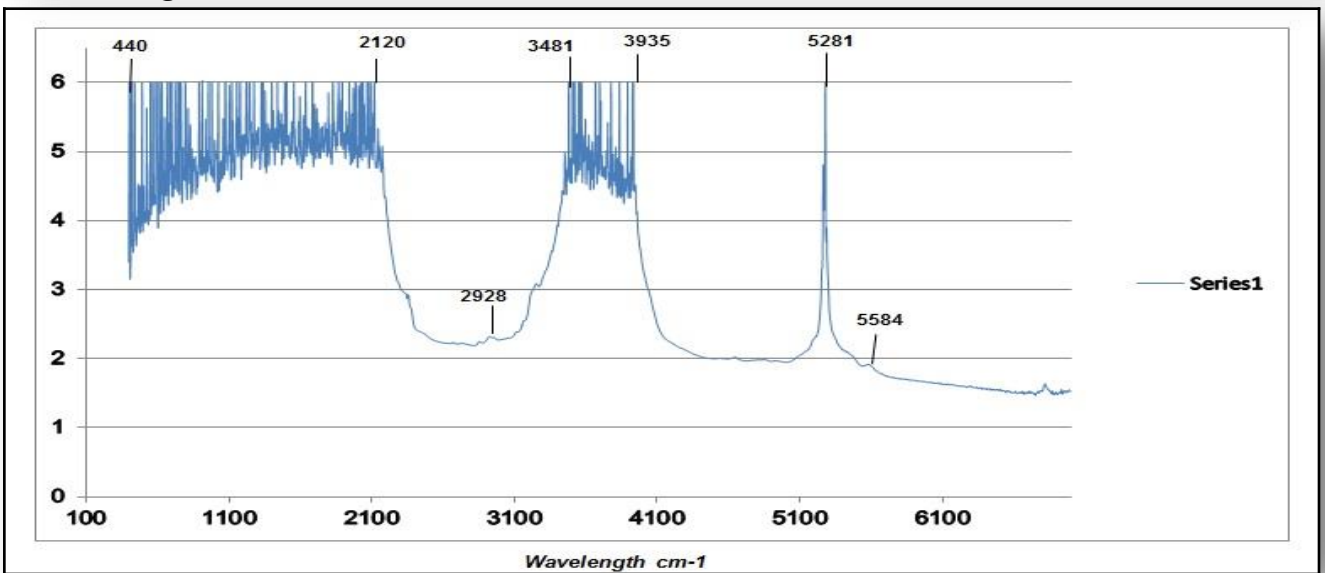
DSK-5 Fig 53
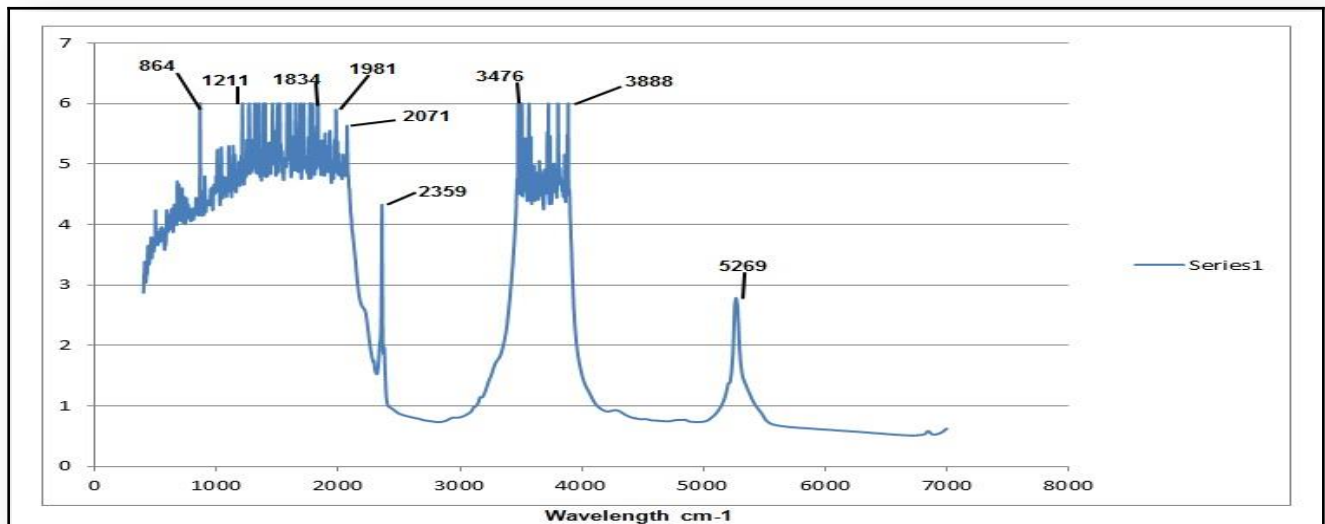
DSK-7 Fig 54
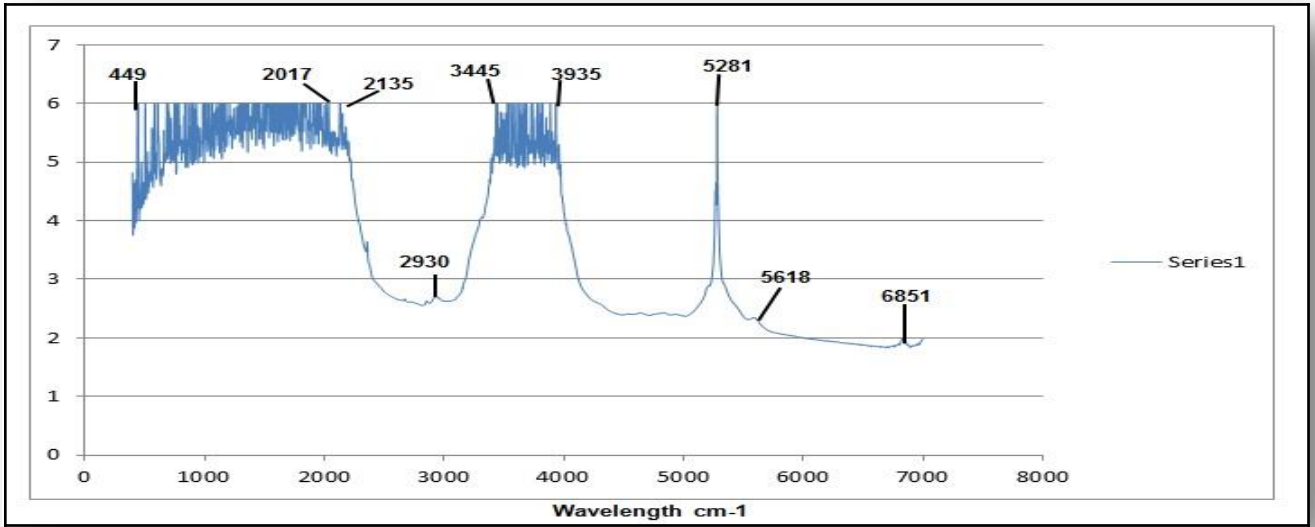
Raman (Bruker MultiRAM)

DSK-1 Fig 55
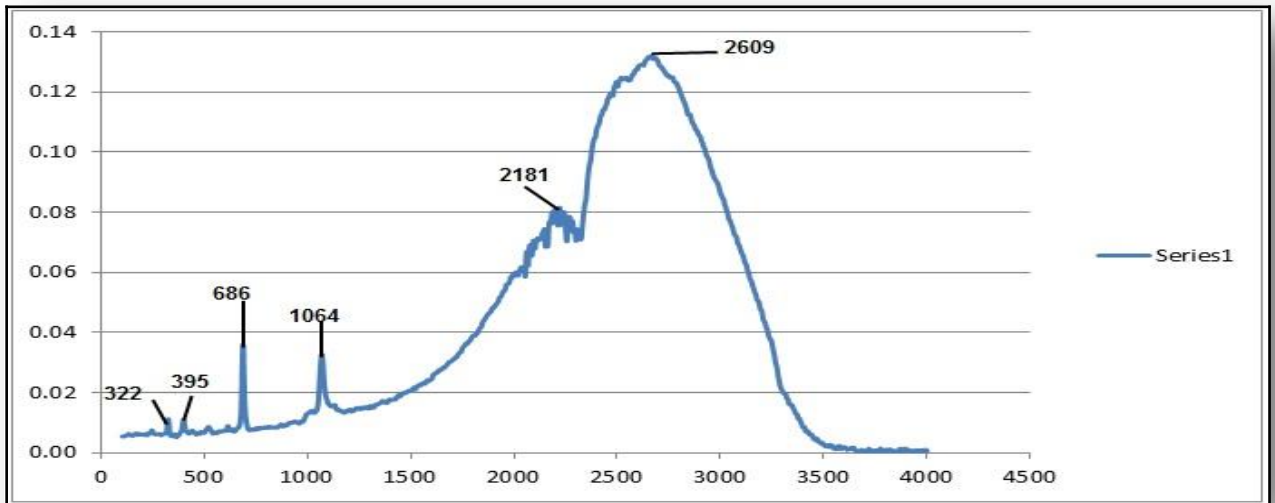
DSK-2 Fig 56
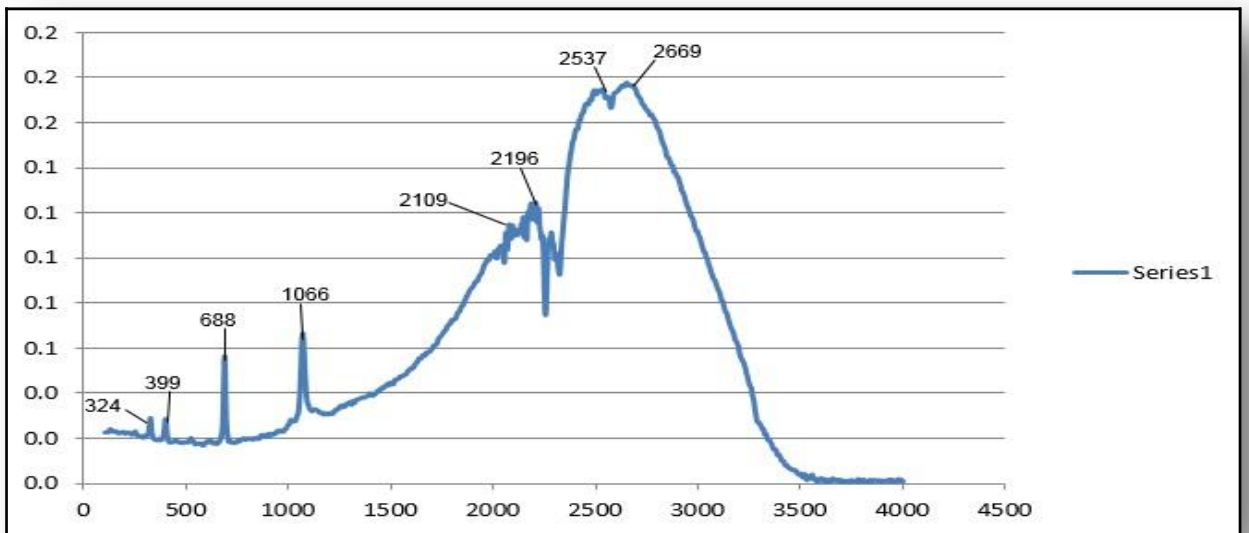
DSK-3 Fig 57
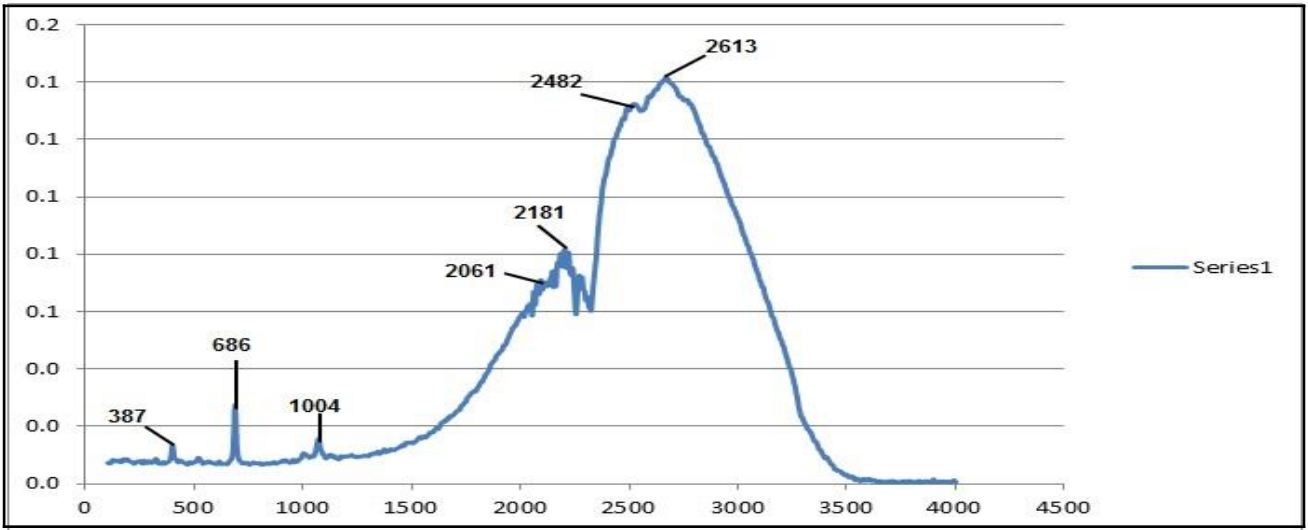
DSK-4 Fig 58
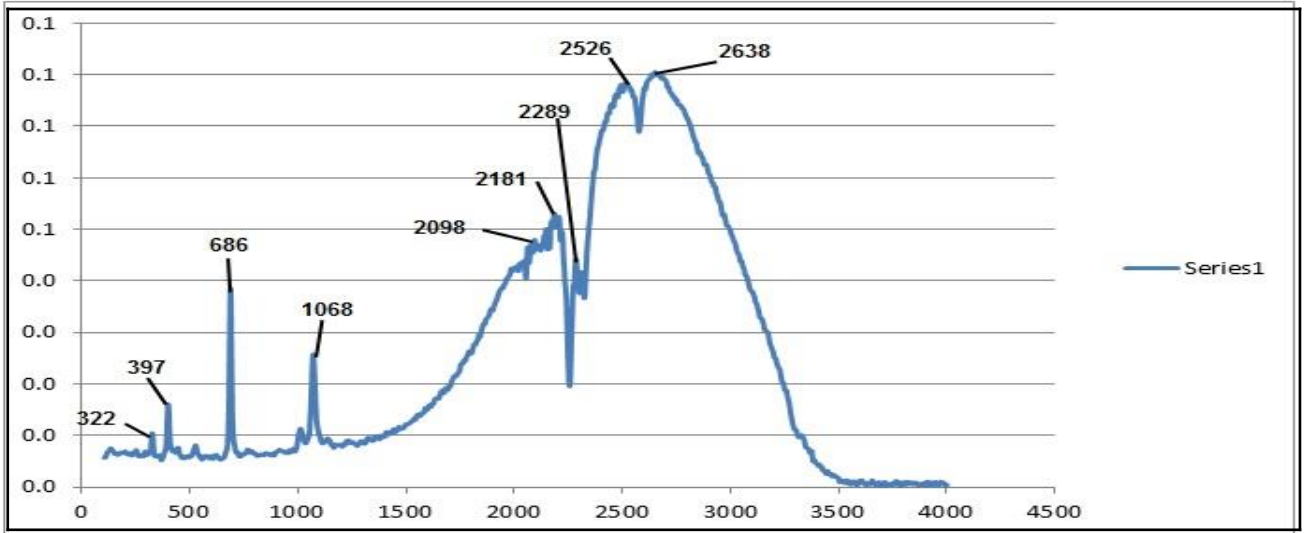
DSK-5 Fig 59
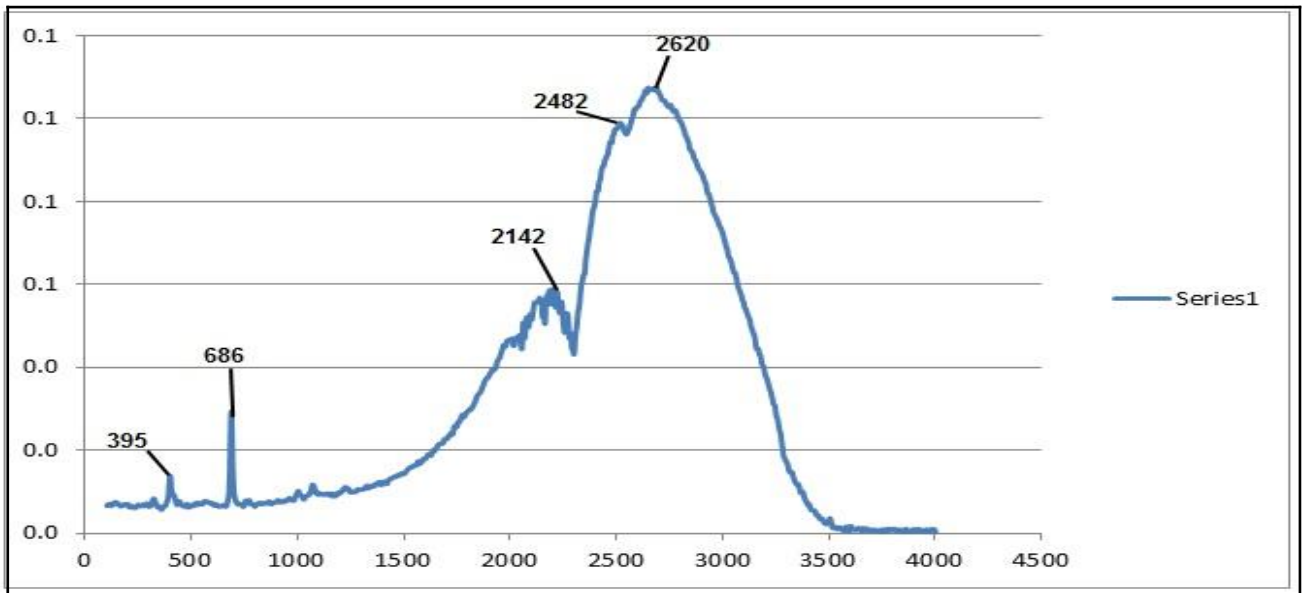
DSK-6 Fig 60
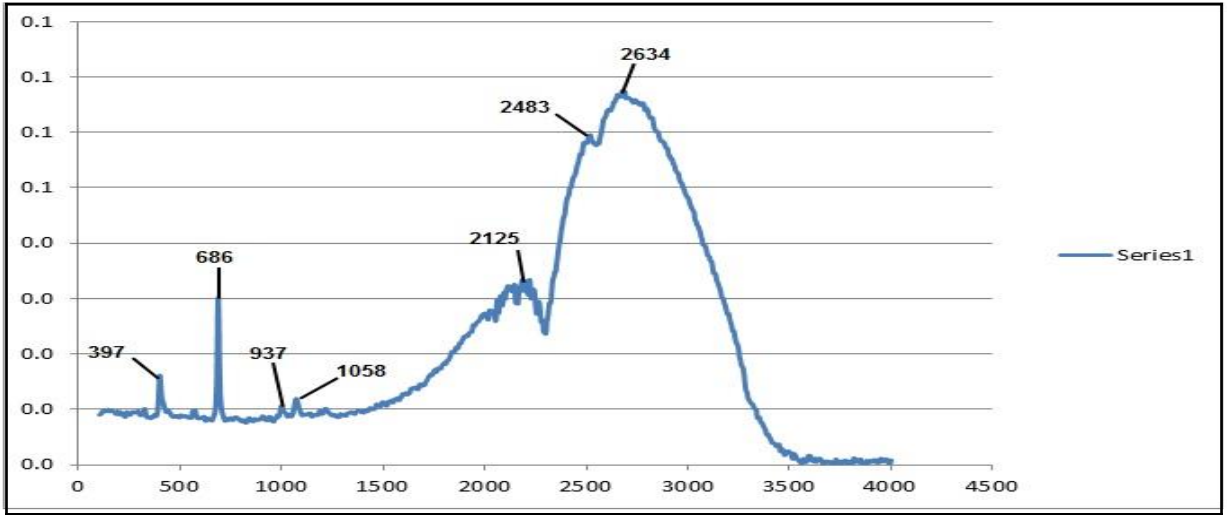
DSK-7 Fig 61
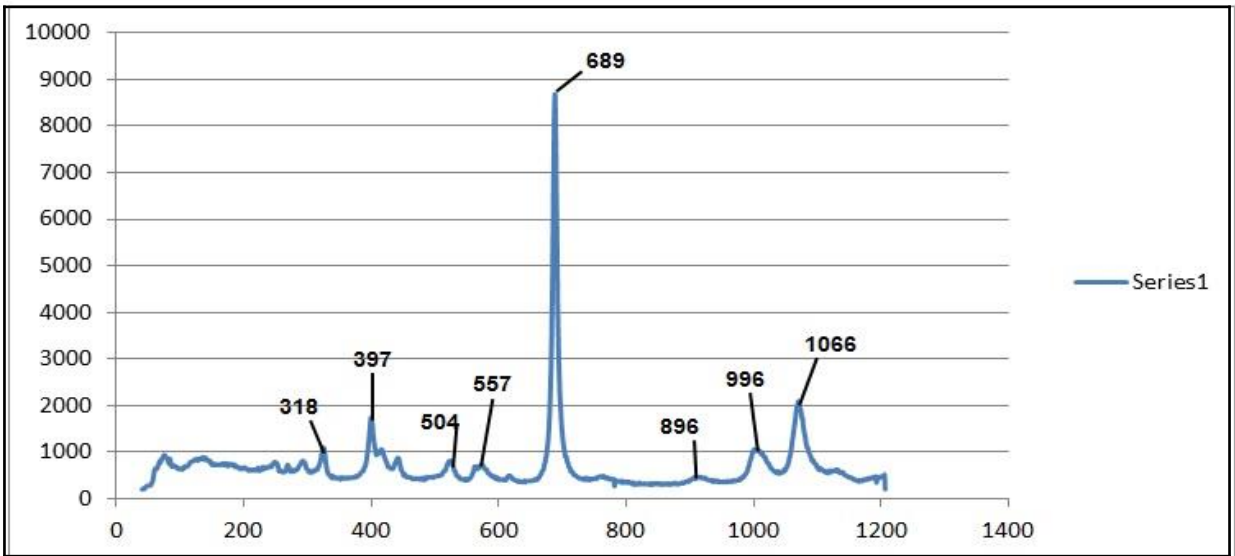
DSK-8 Fig 62
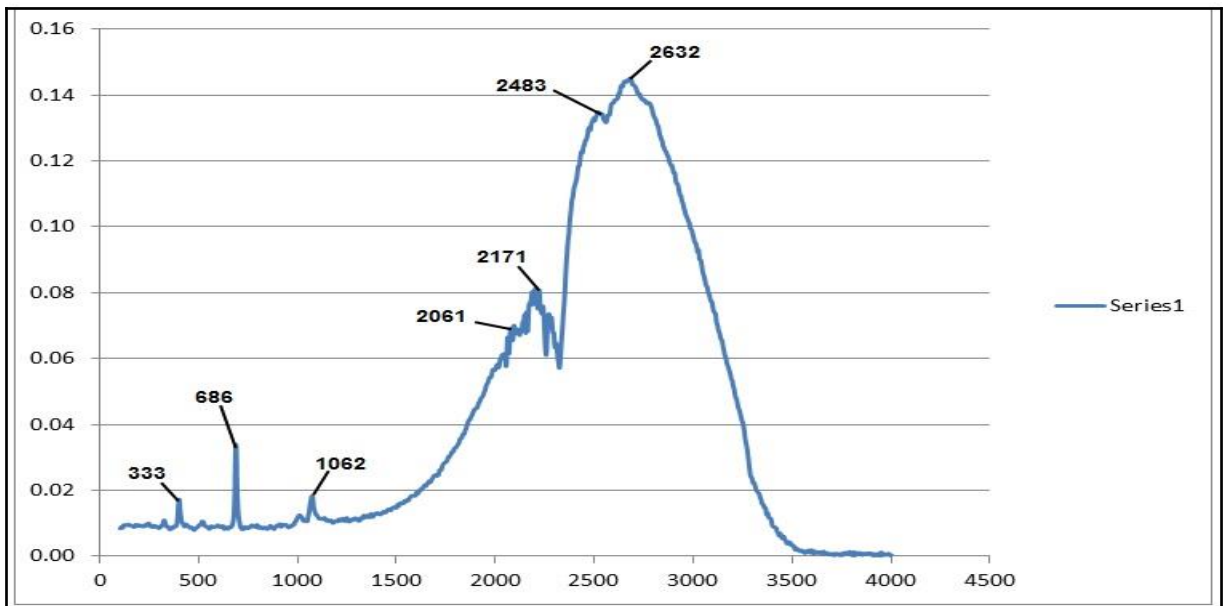
4D. Raman Microprobe HORIBA T64000

DSK-1 63
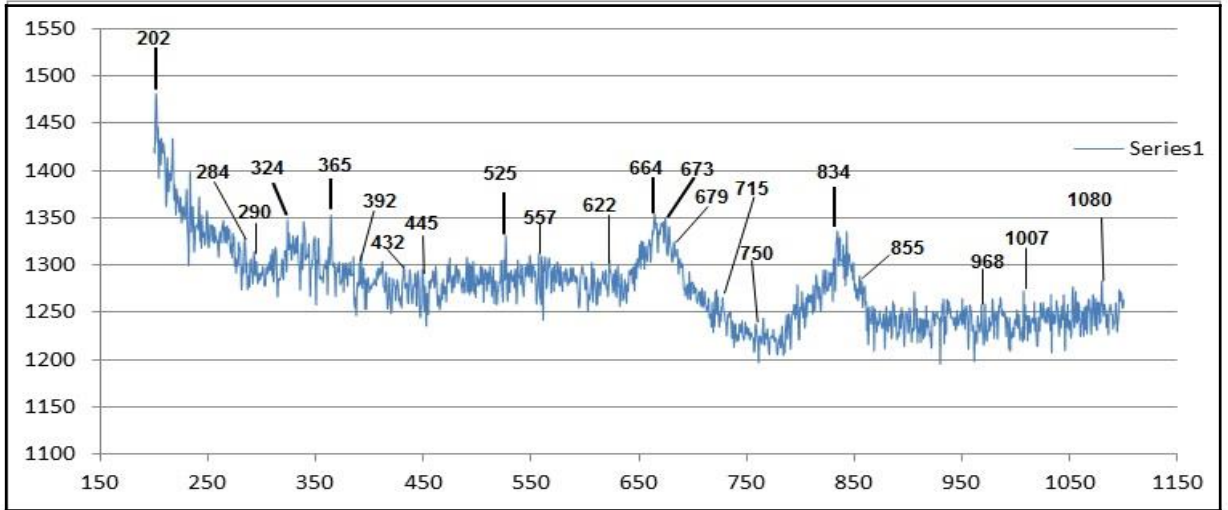
DSK-1 Fig 64
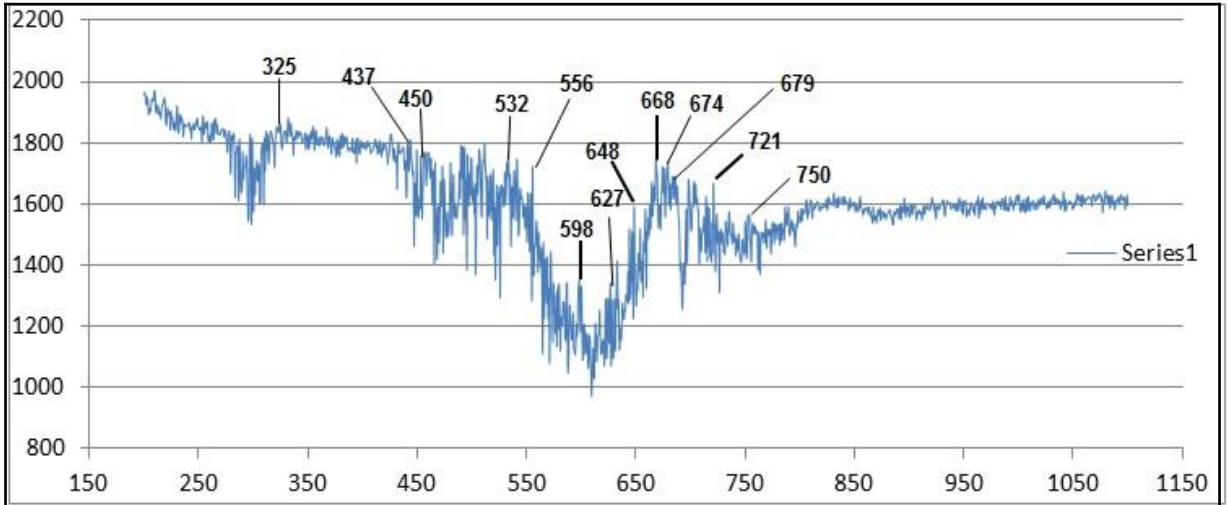
DSK-2 Fig 65
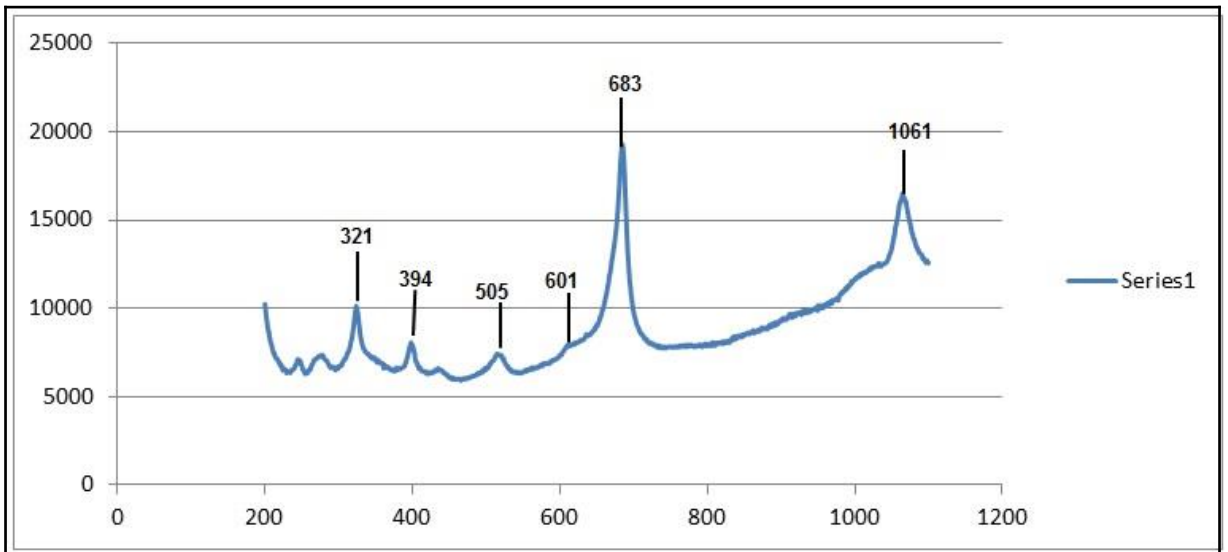
DSK-2 Fig 66
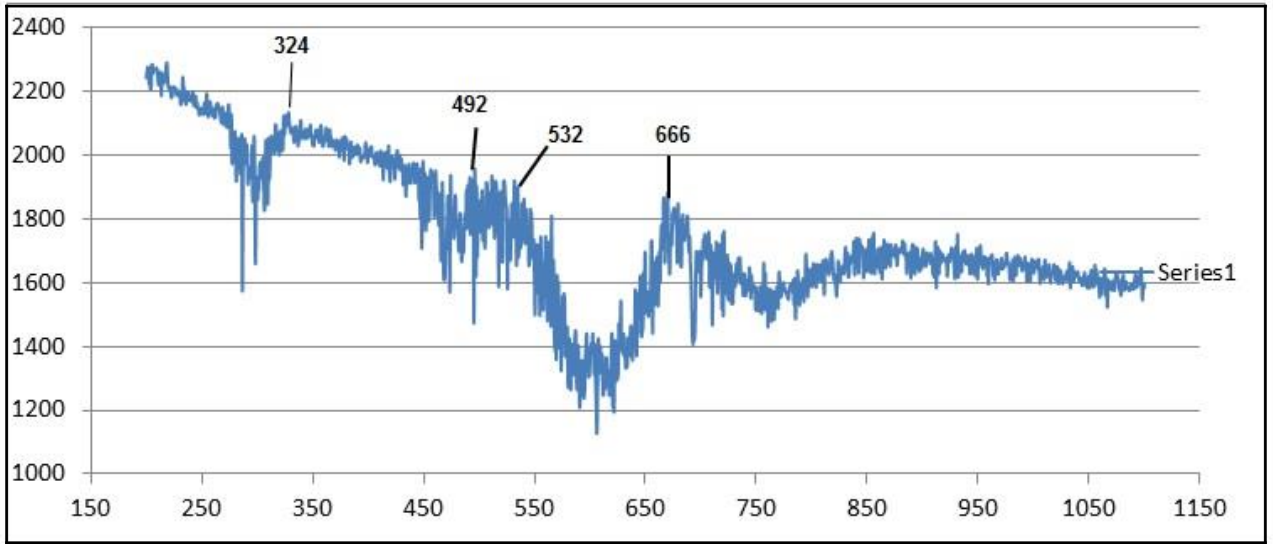
DSK-3 Fig 67
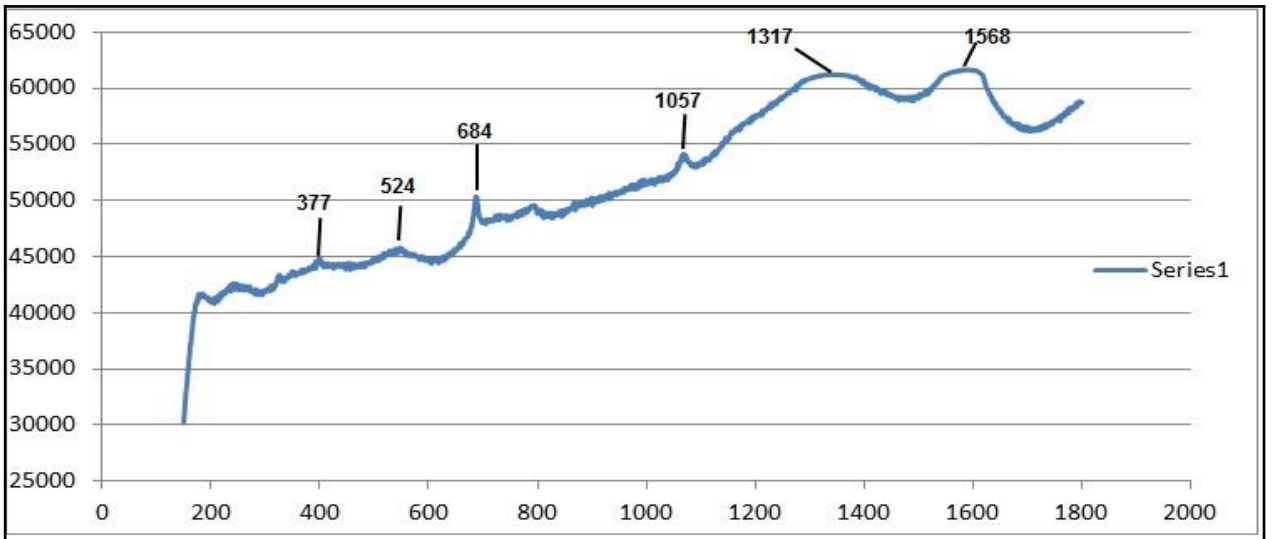
DSK-3 Fig 68
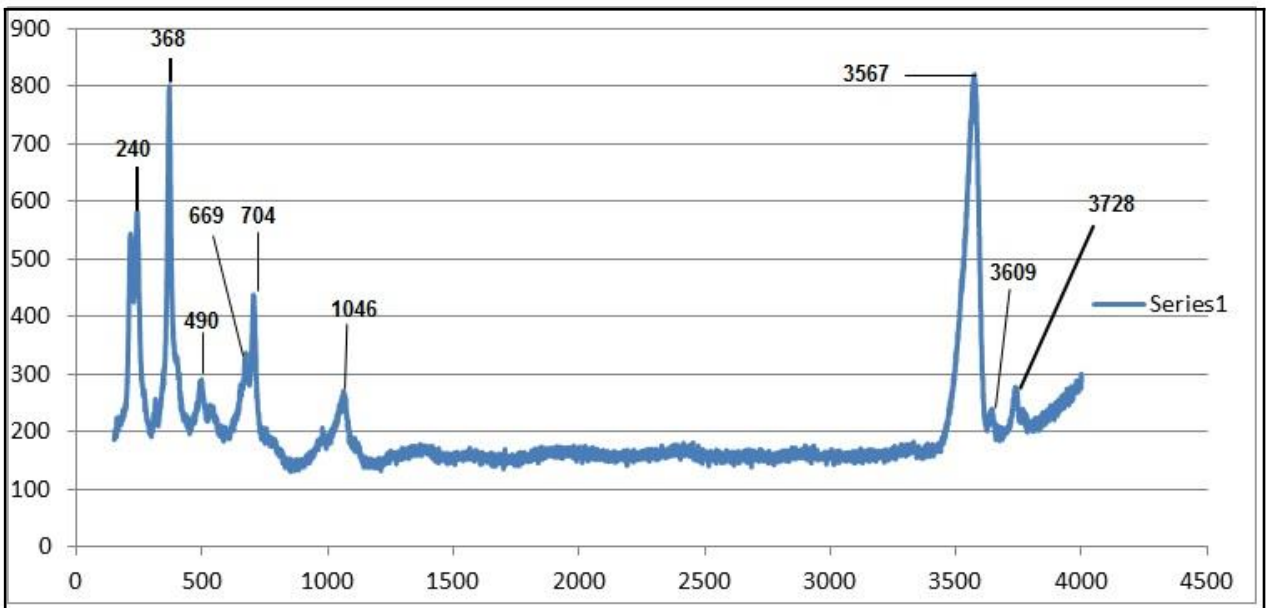
DSK-3 Fig 69
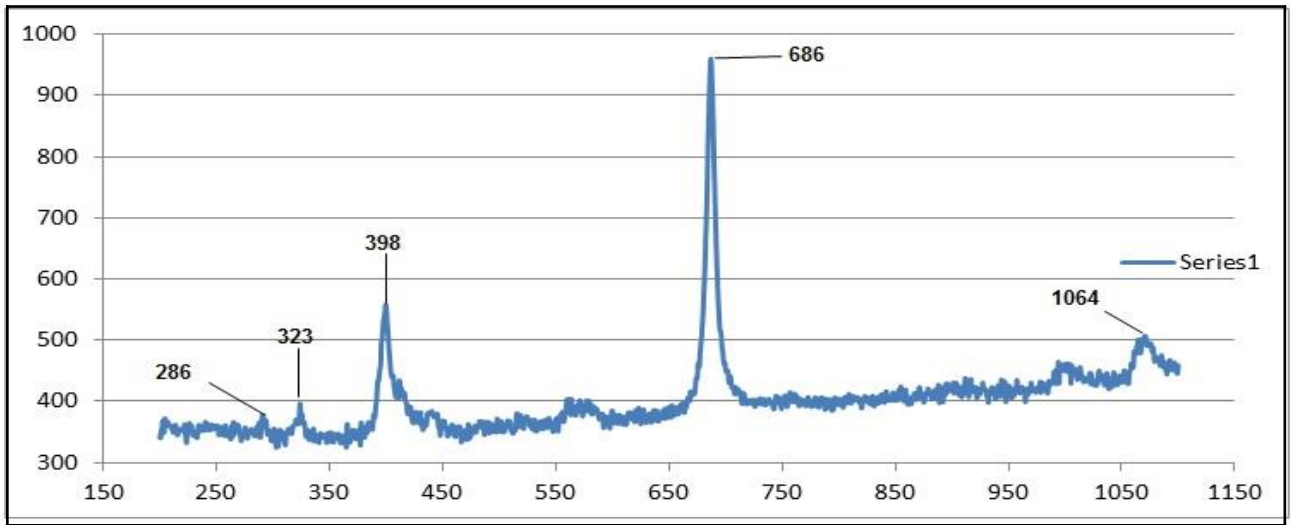
DSK-6 Fig 70
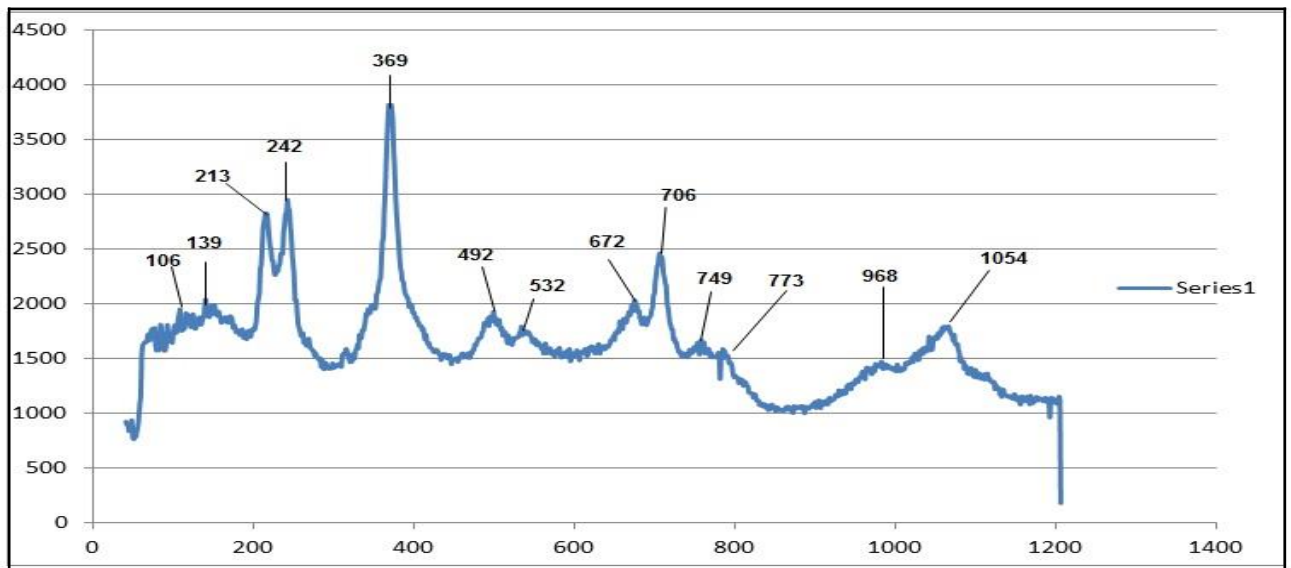
DSK-6 Fig 71
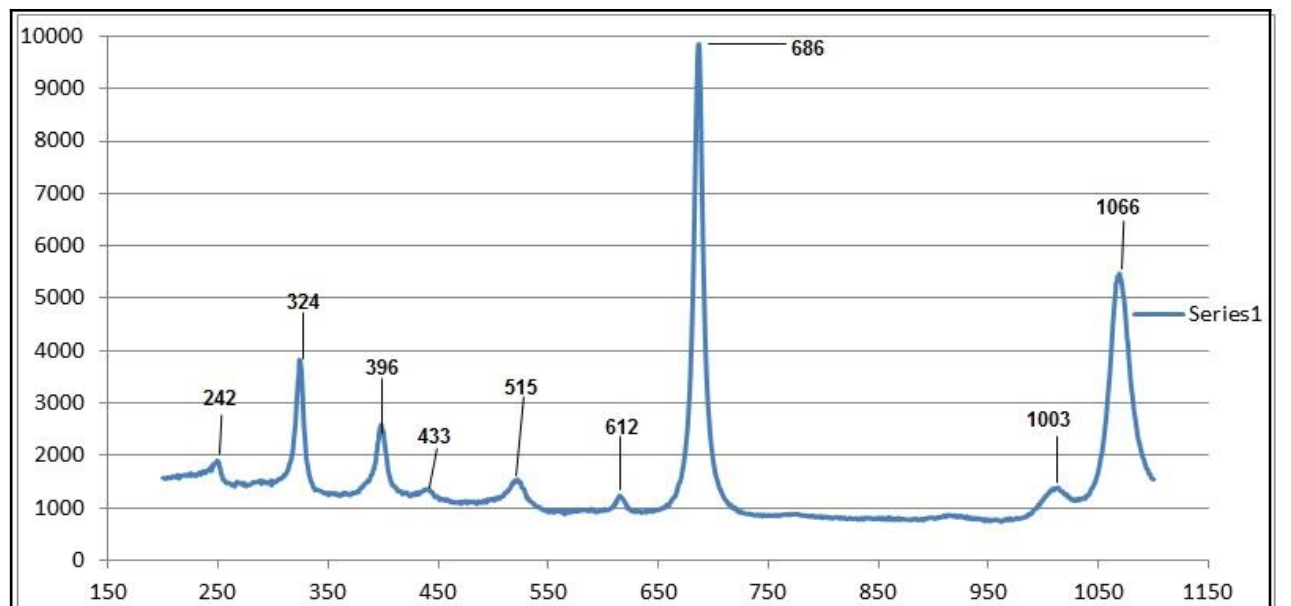
4E. Raman spectrometer, LabramHR

DSK-5 72
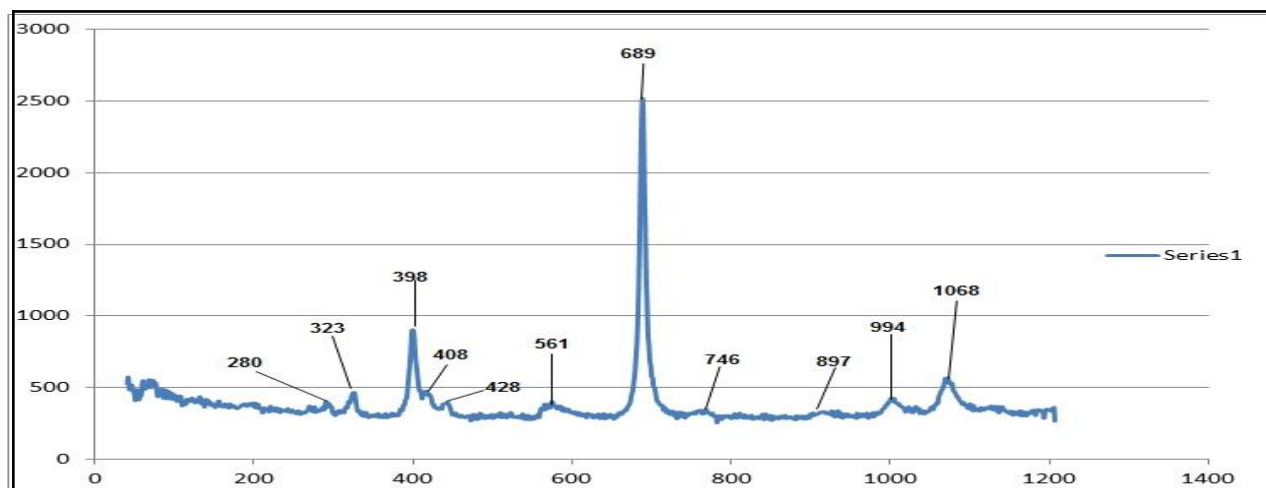
DSK-5 Fig 73
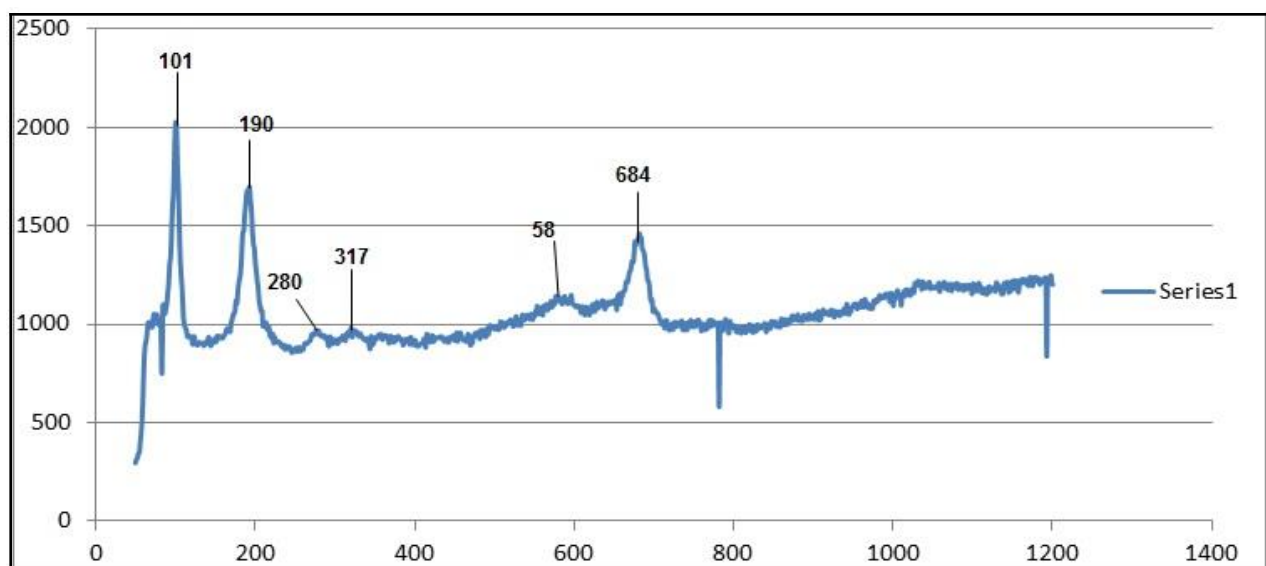
DSK-6 Fig 74
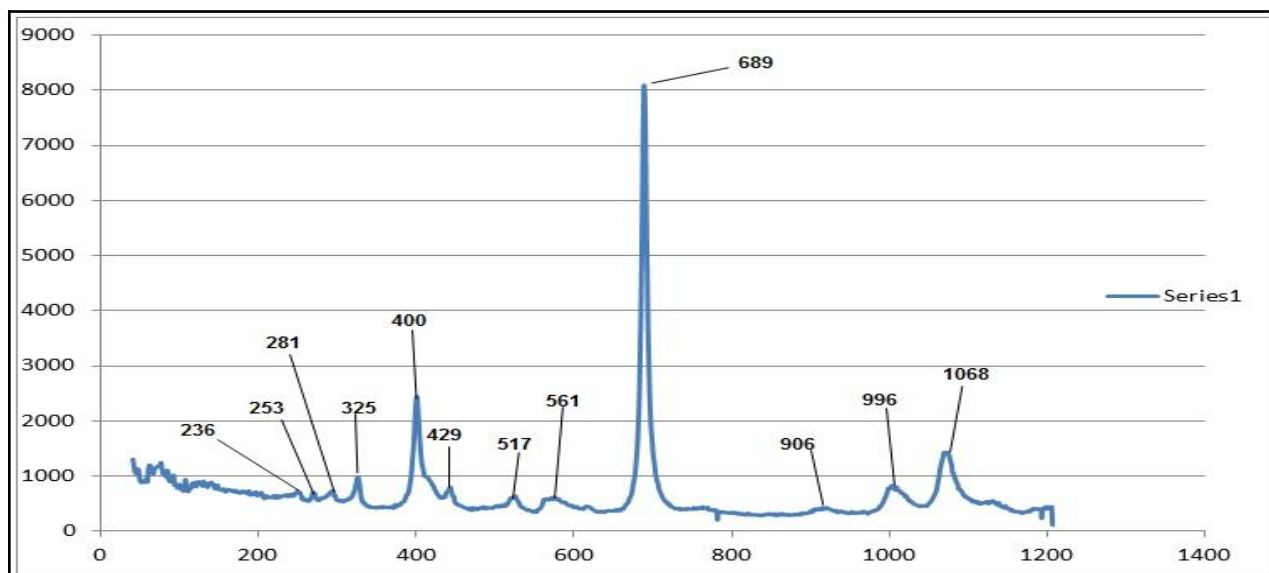
DSK-6 Fig 75
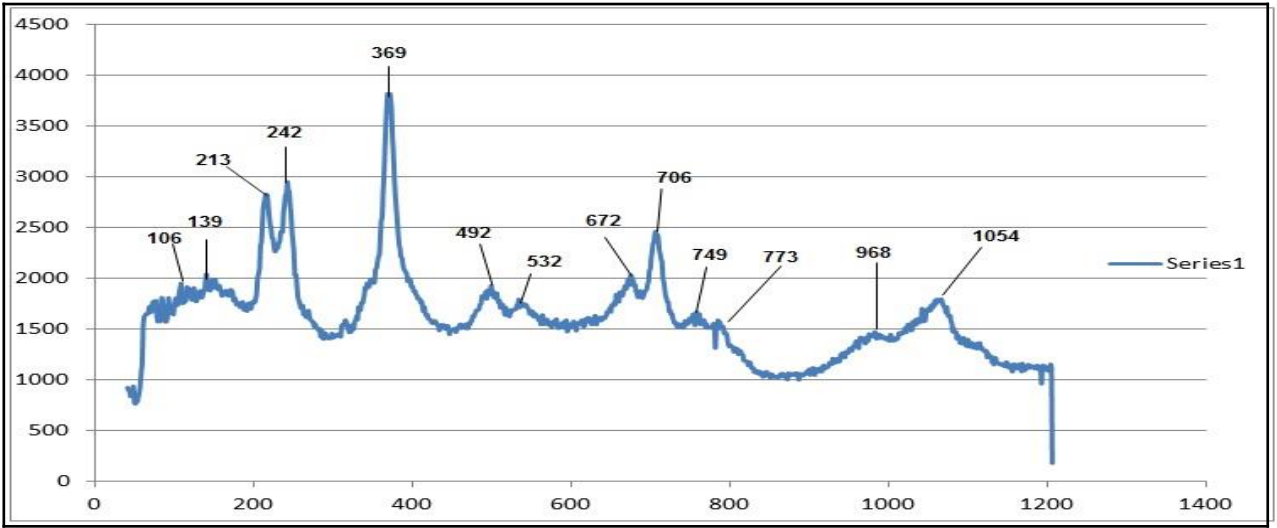
DSK-6 Fig 76
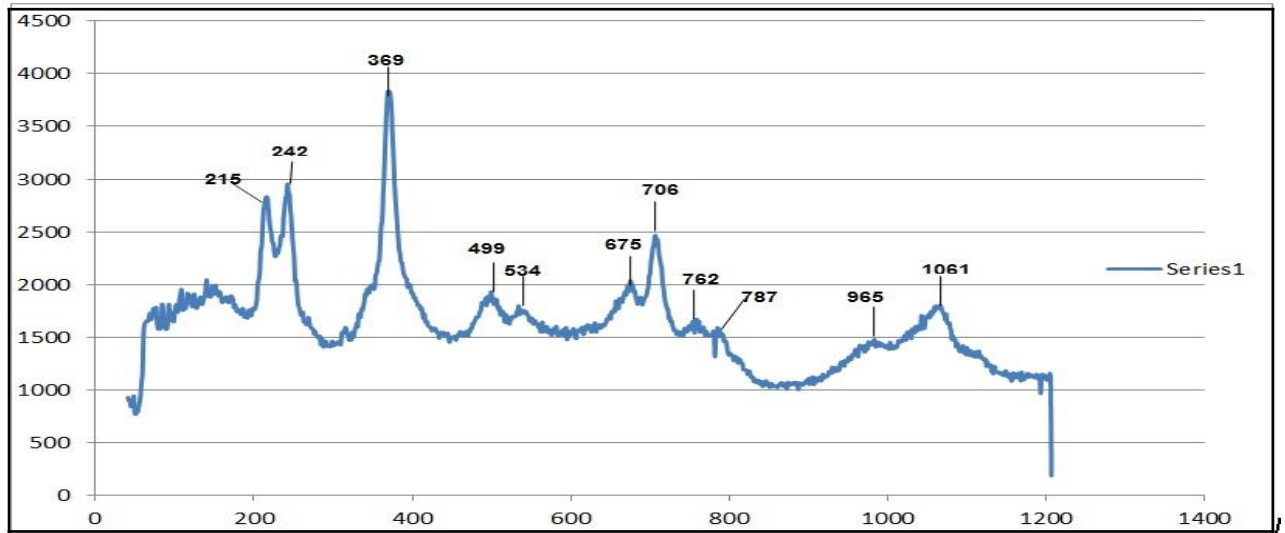
DSK-6 Fig 77
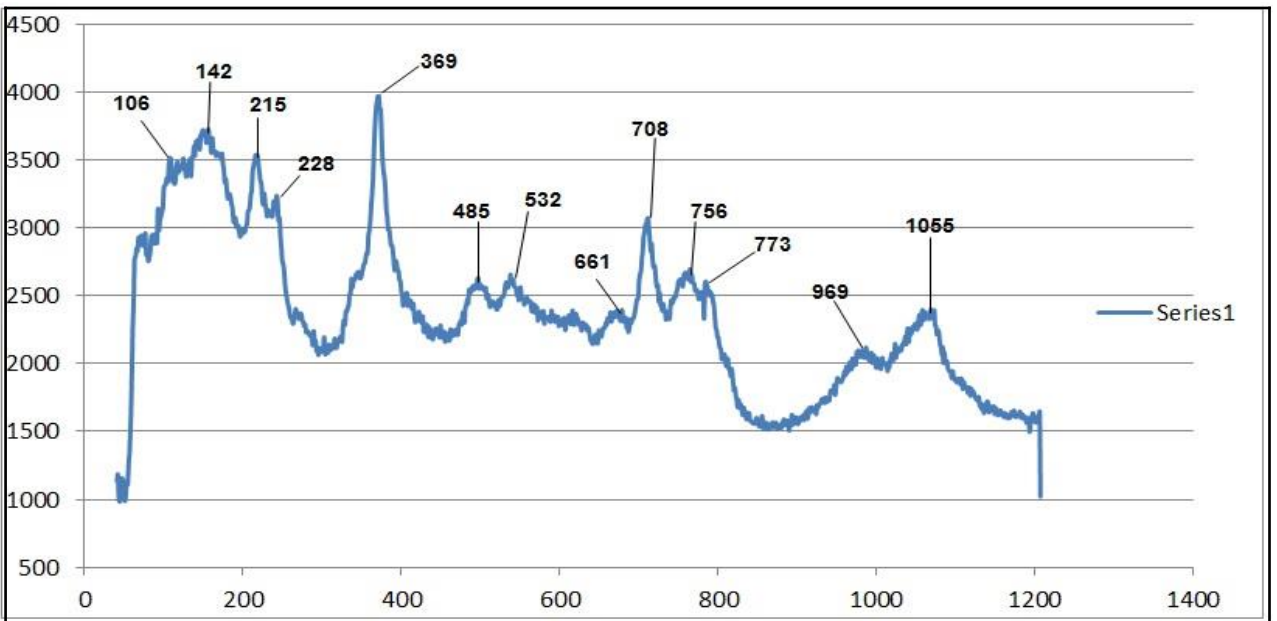
DSK-7 Fig 78
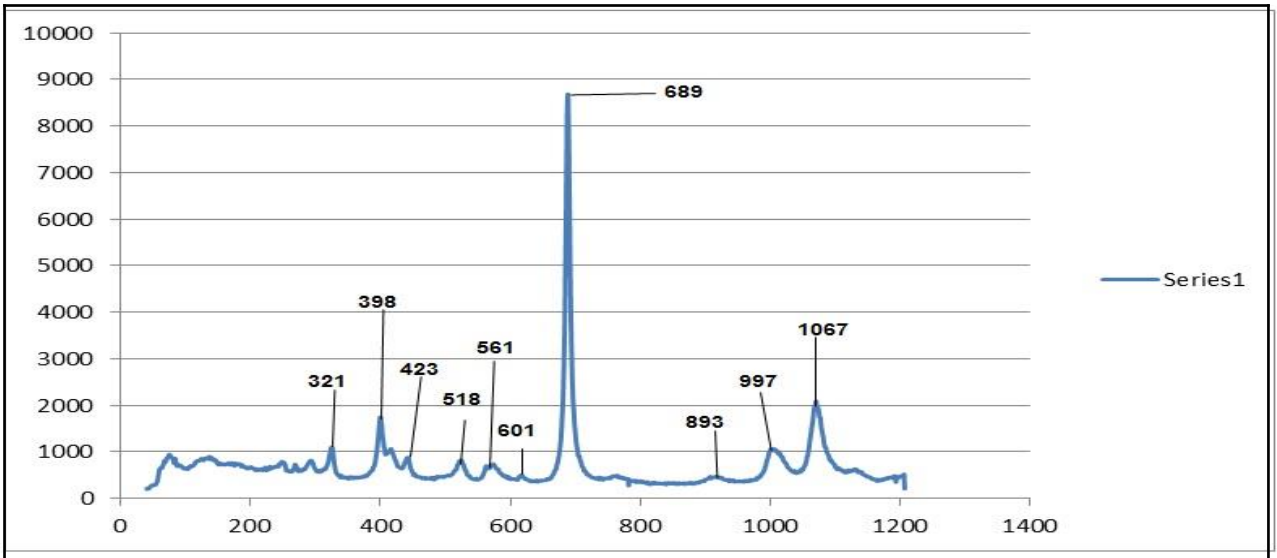
DSK-7 Fig 79
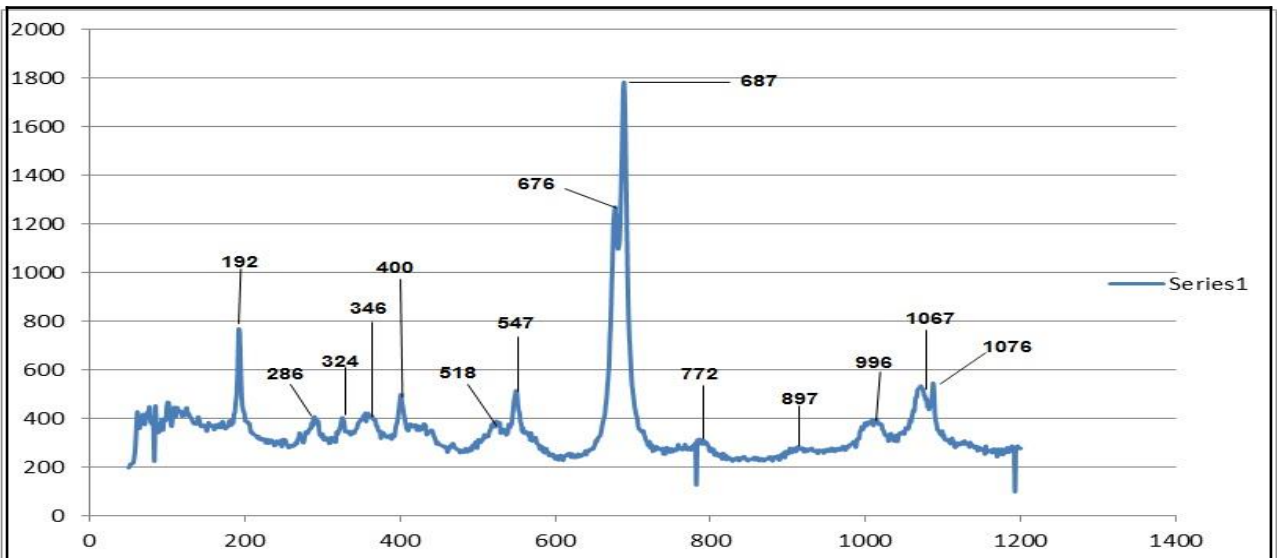
4E. RAMAN STR-300 (GTL, Japipur)

DSK 1a Fig 80
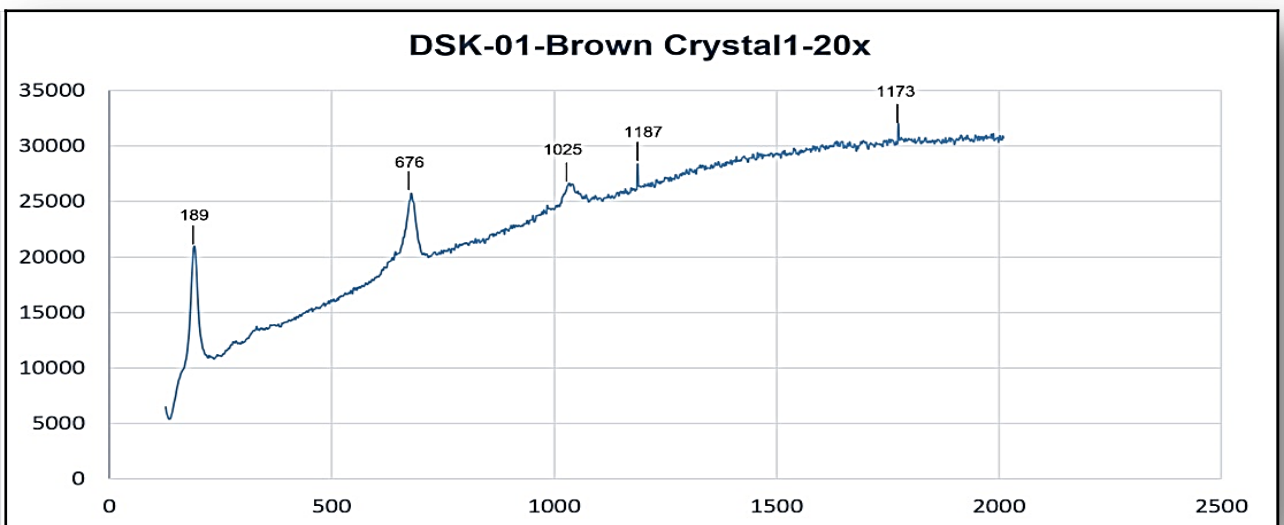
DSK 1b Fig 81
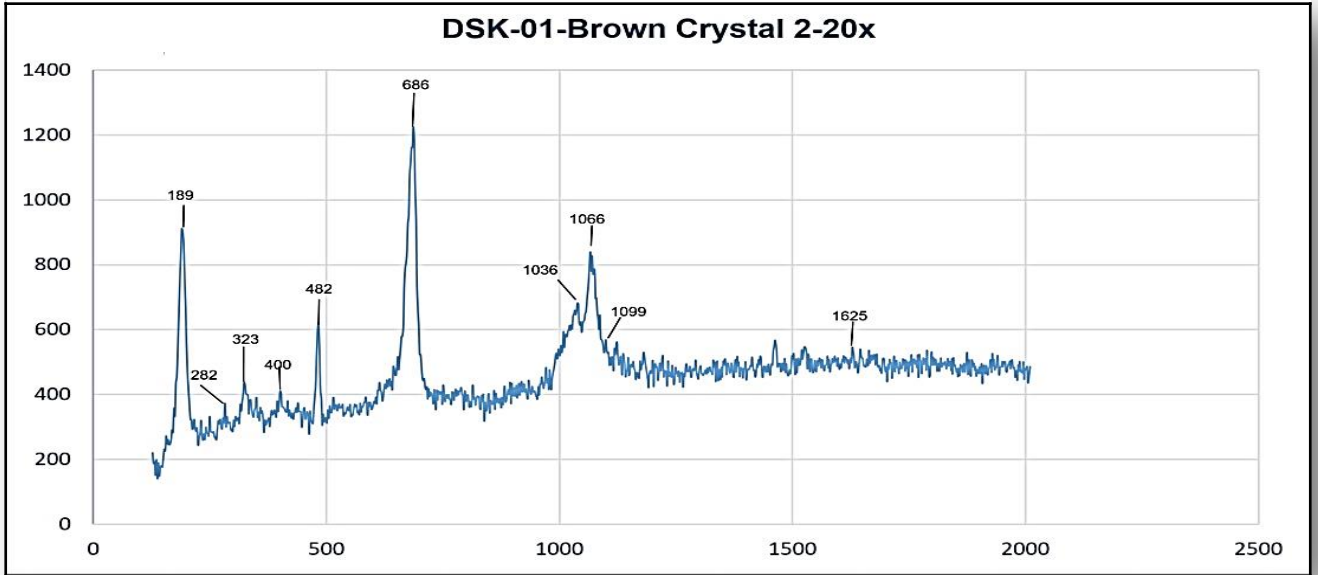
DSK-01-Brown Crystal 2-20x
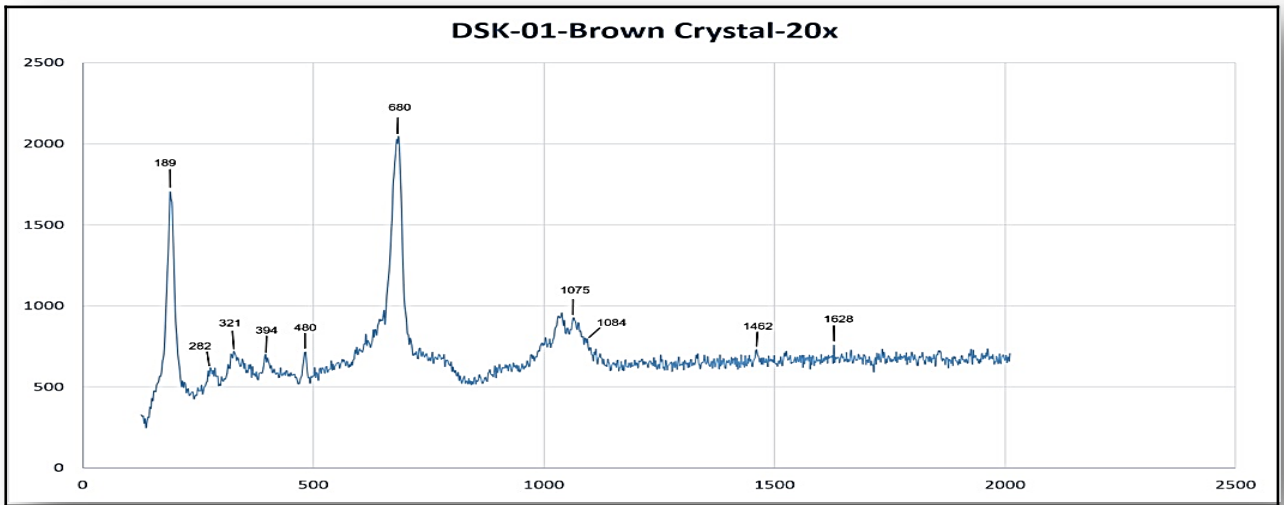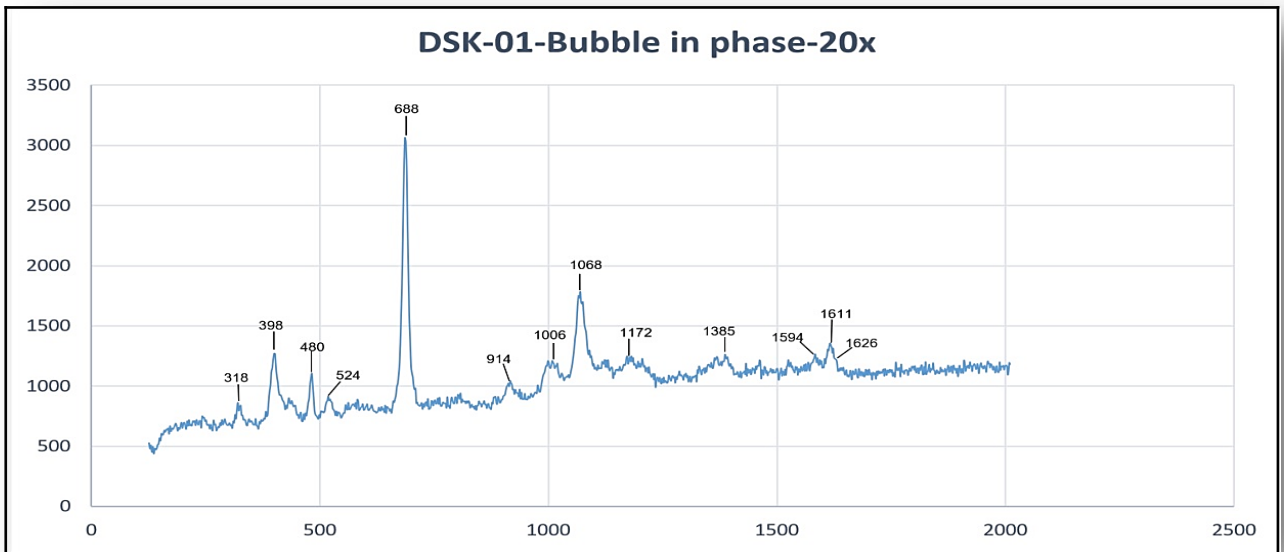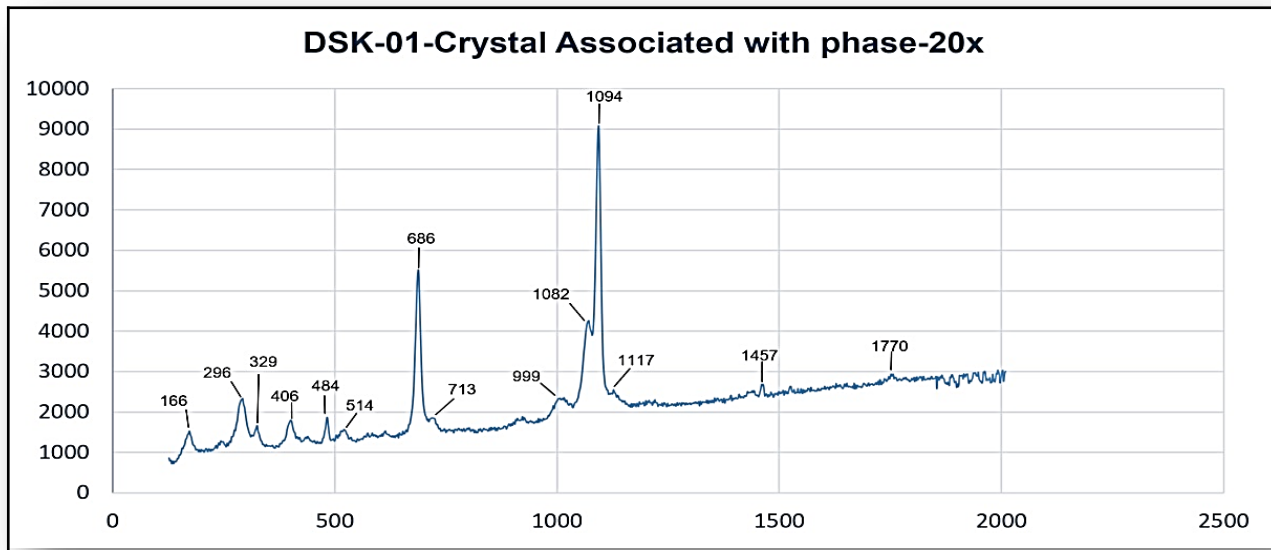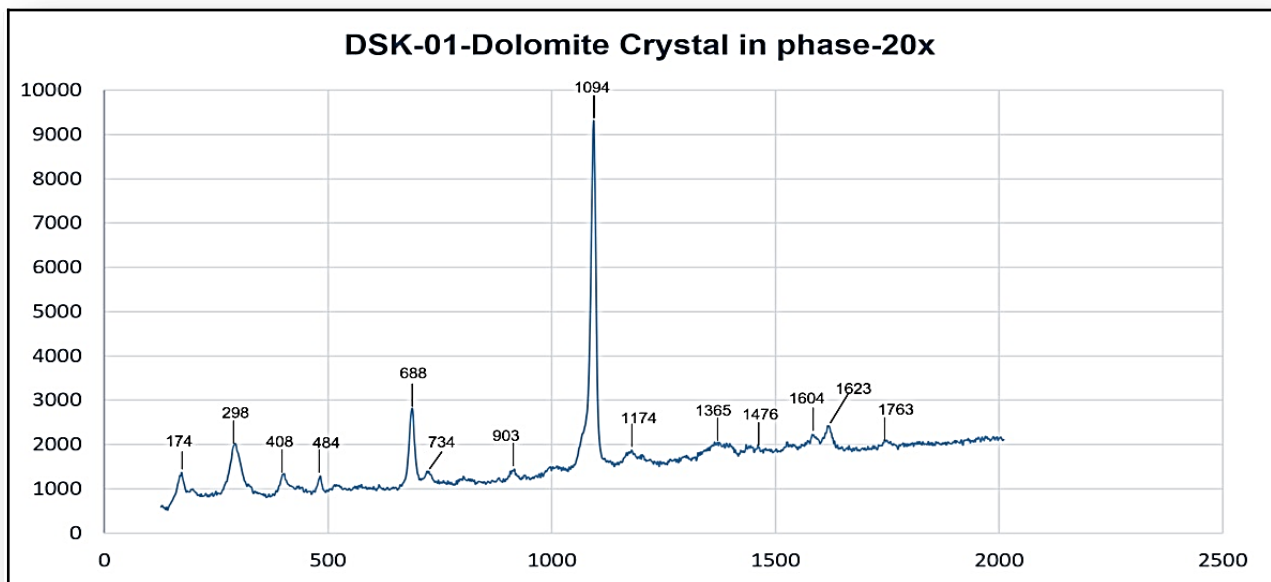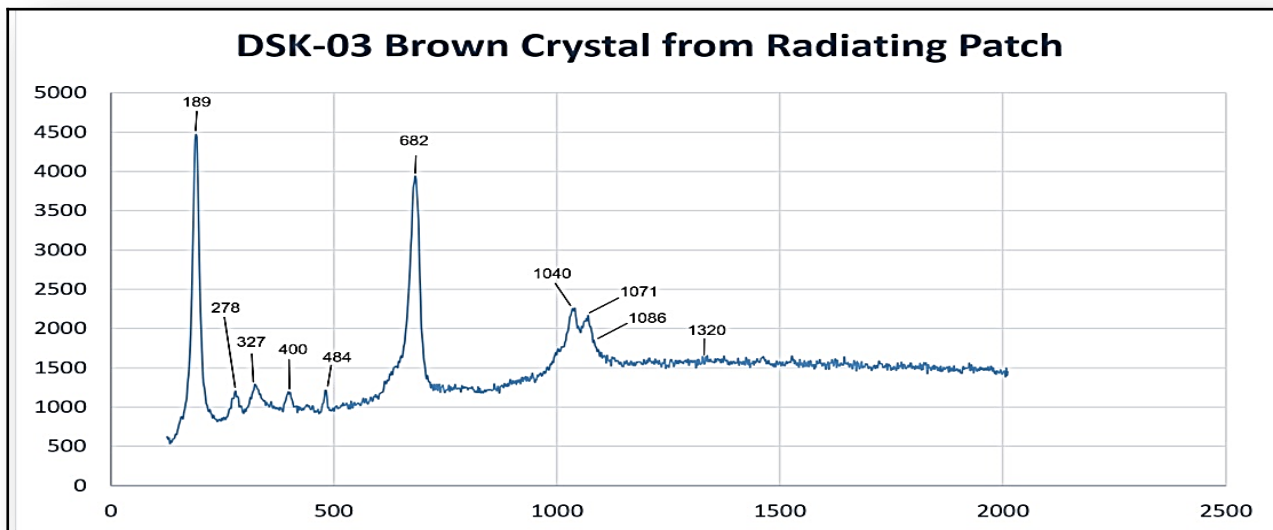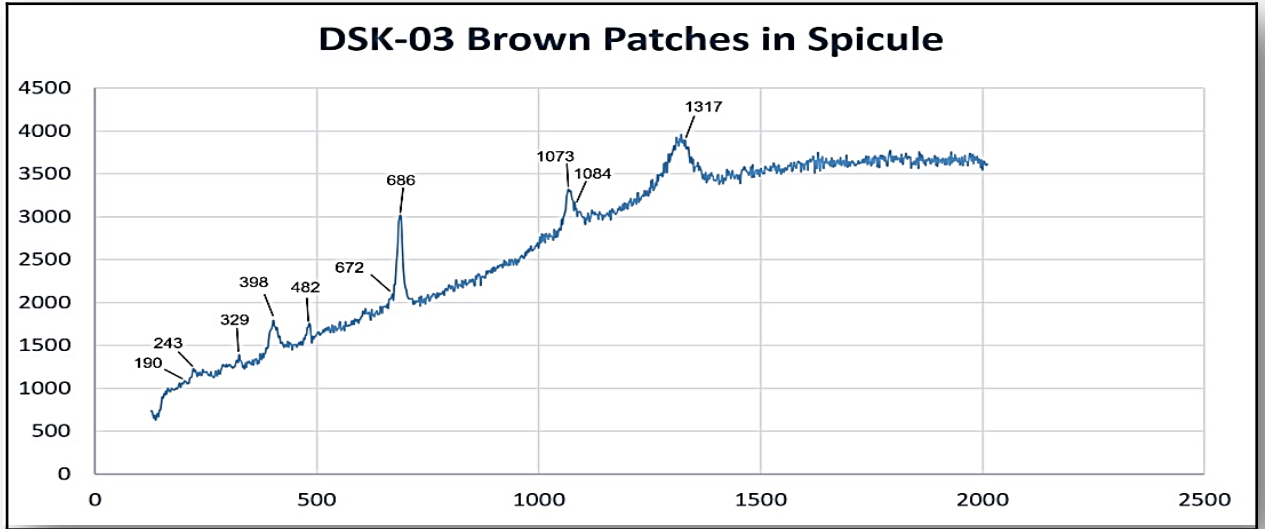
DSK 1c Fig 82

DSK-01-Brown Crystal-20x

DSK 1d Fig 83

DSK-01-Bubble in phase-20x

DSK 1e Fig 84

DSK-01-Crystal Associated with phase-20x

DSK 1f Fig 85

DSK-01-Dolomite Crystal in phase-20x

DSK 3a Fig 86

DSK-03 Brown Crystal from Radiating Patch

DSK 3b Fig 87

DSK-03 Brown Patches in Spicule

DSK 3c Fig 88

DSK-03 Calcite in Spicule

DSK 3d Fig 89

DSK-03 Curved Needle

DSK 3e Fig 90

DSK-03 Dark Brown Crystal Patch

DSK 6a Fig 91

DSK-06 Dark Blue-Black Tourmaline

DSK 6b Fig 92

DSK-06 Orange-Brown Platelet-Hematite

DSK-08 Crystal-Side-Overlap with Small Table

DSK 8b Fig 94

DSK-08 Crystal-Side-Small Overlap on Big- Table

DSK 8c Fig 95

DSK-08 Long Crystal-Table
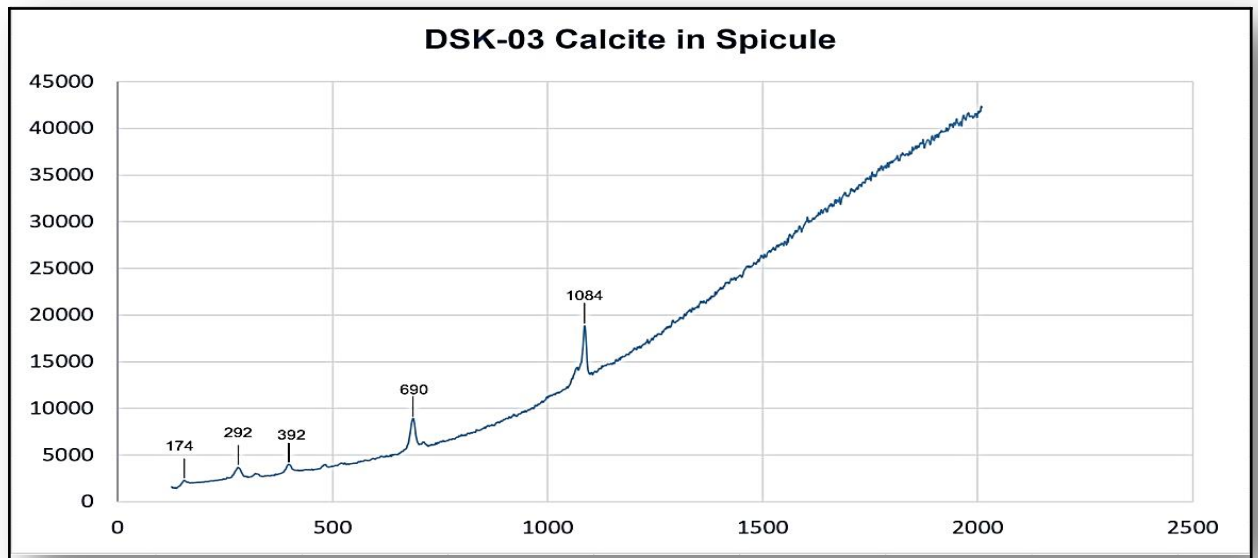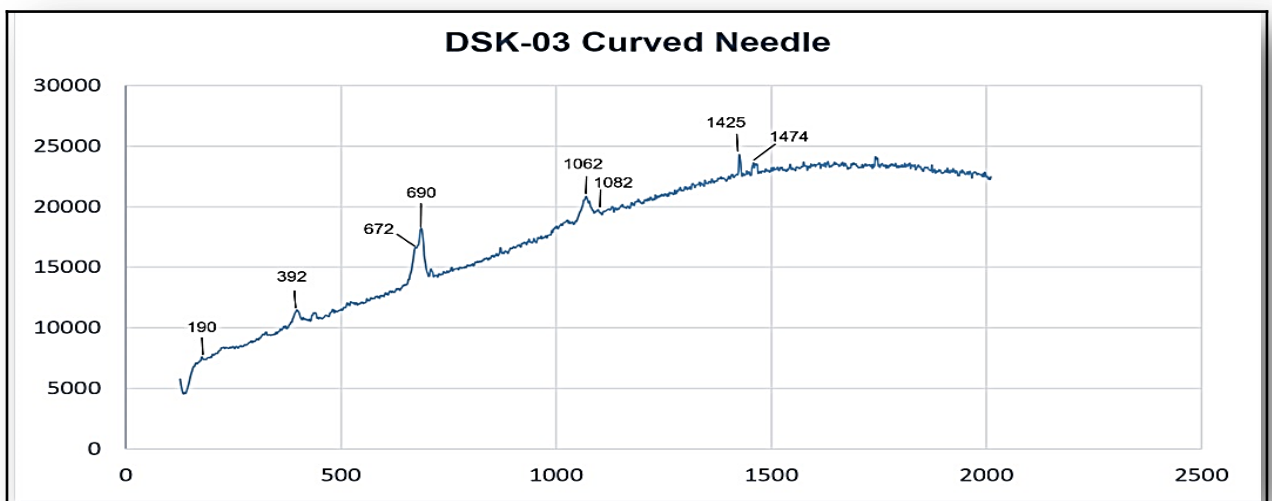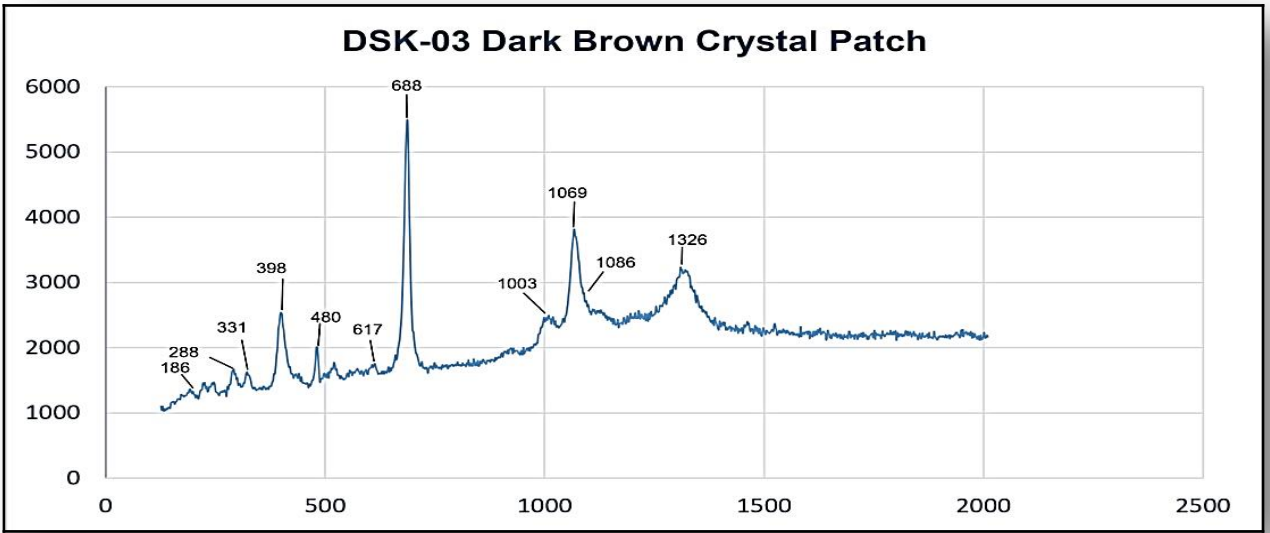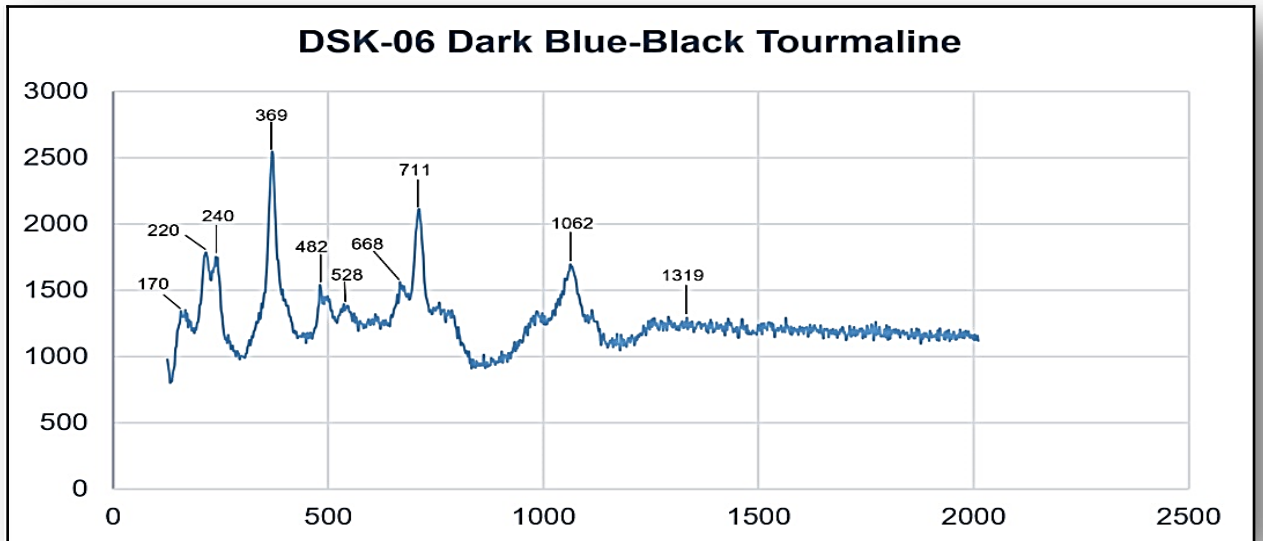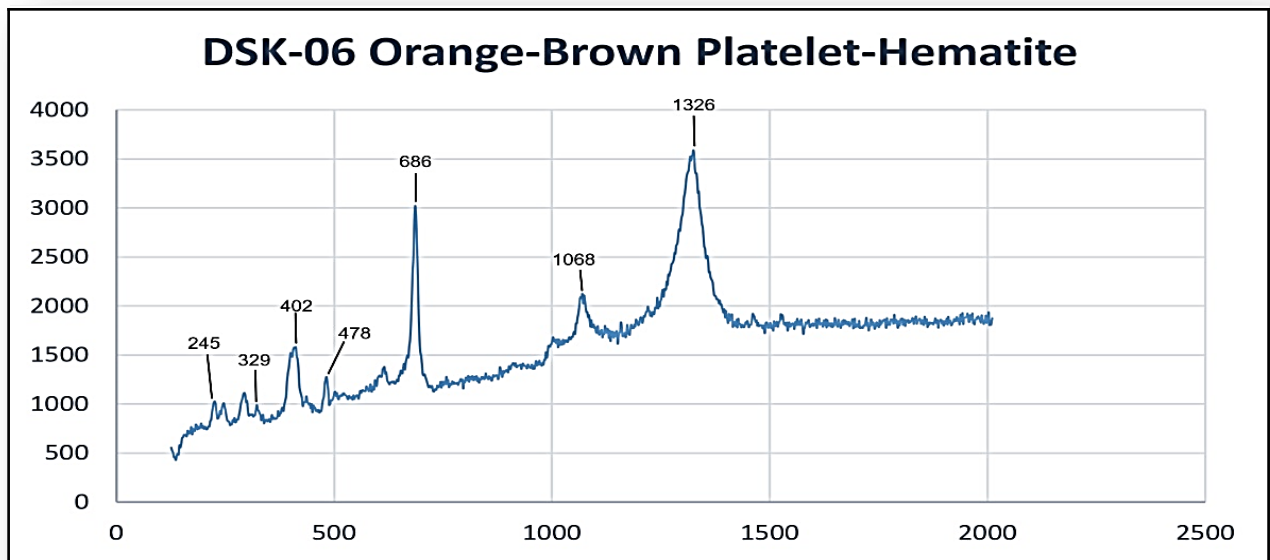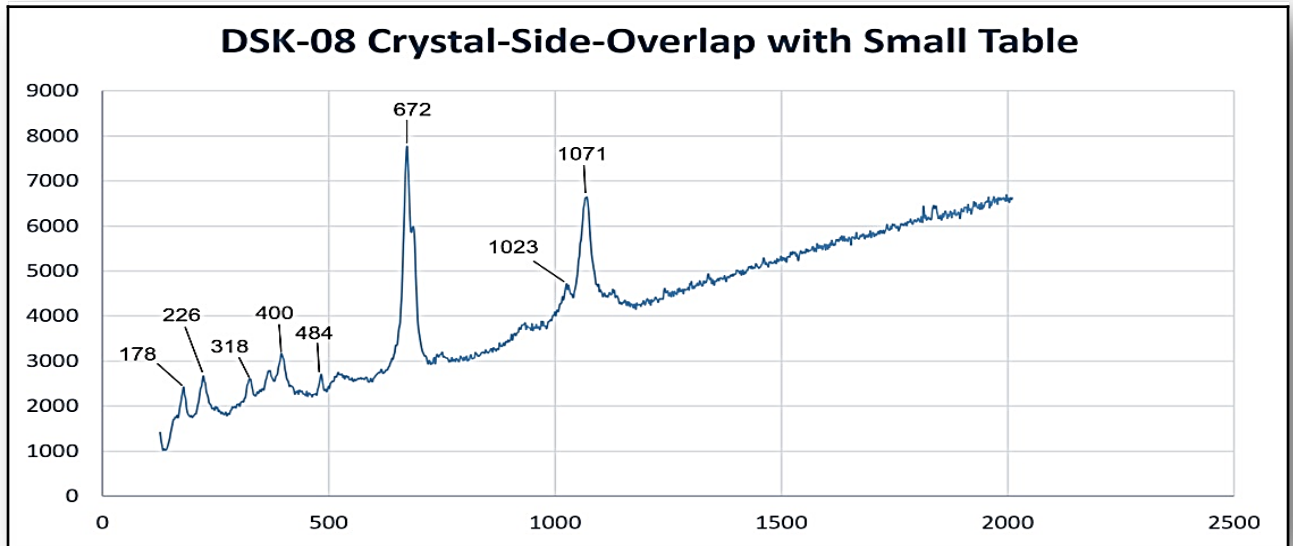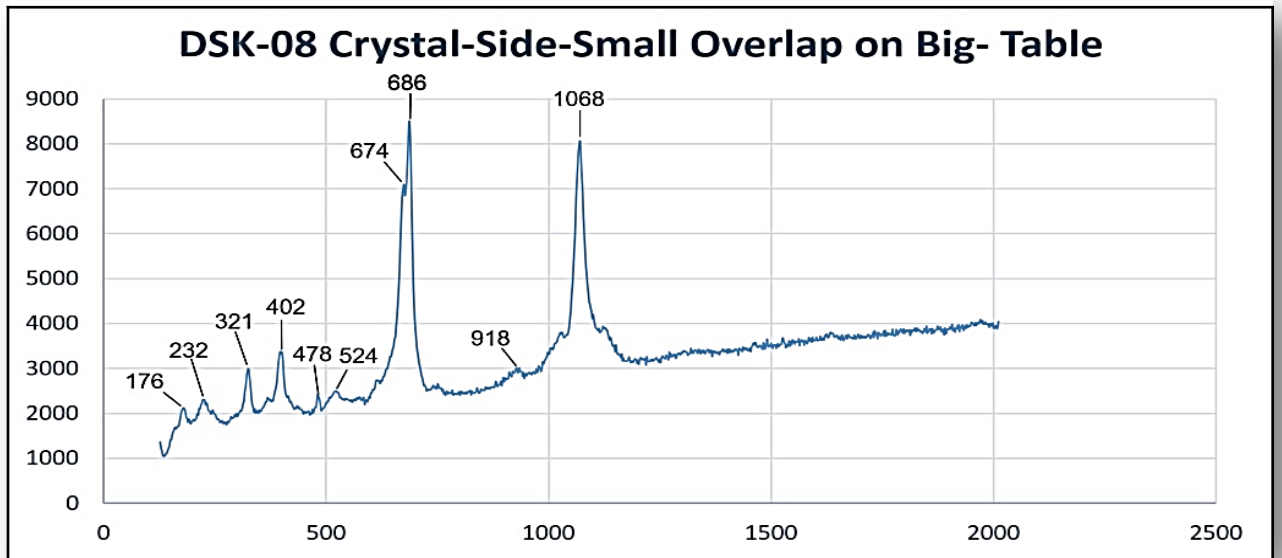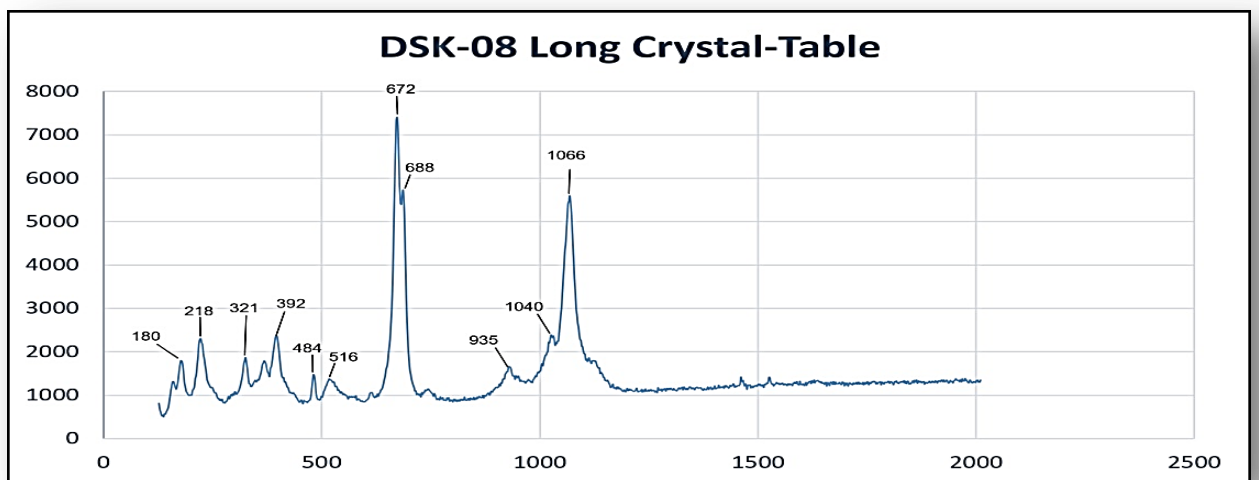
4F. UV-Vis-Spectrometer

DSK-1 Fig 96
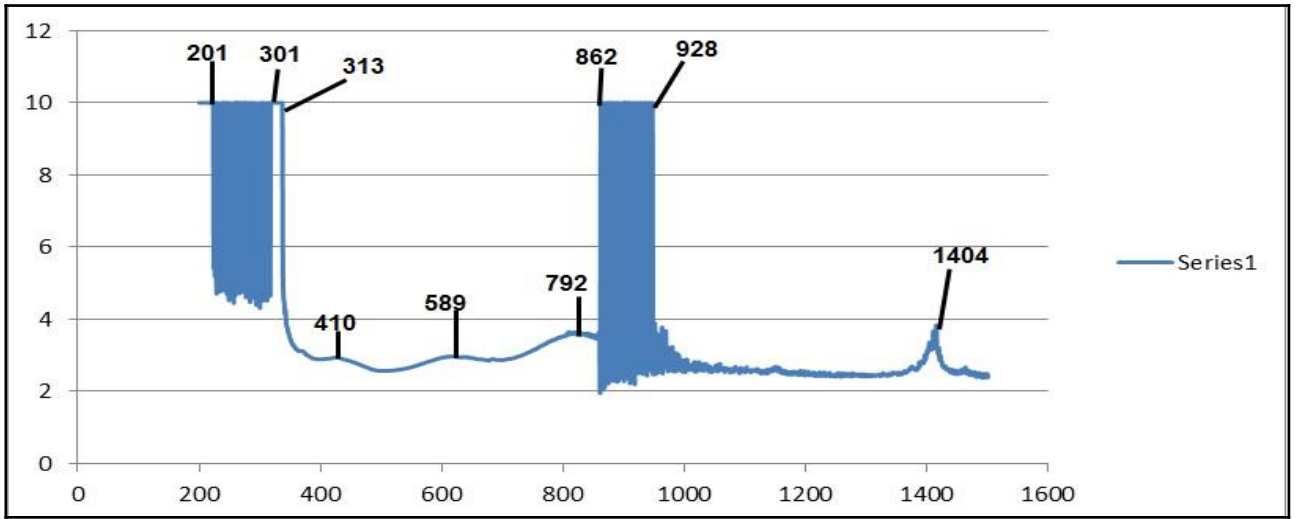
DSK-1 Fig 97
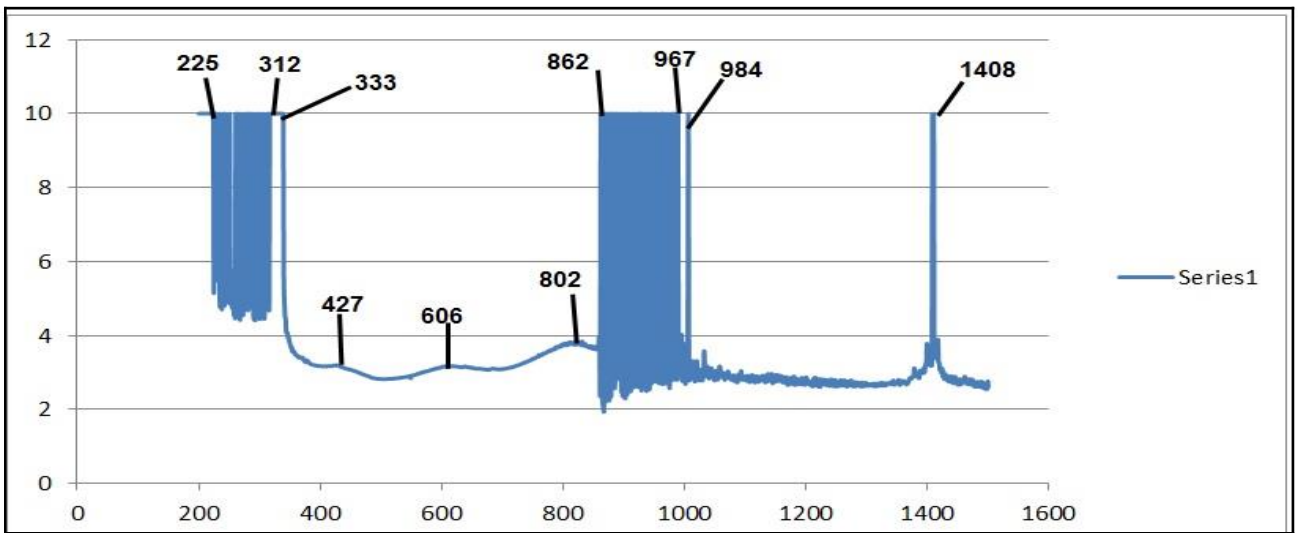
DSK-2 Fig 98
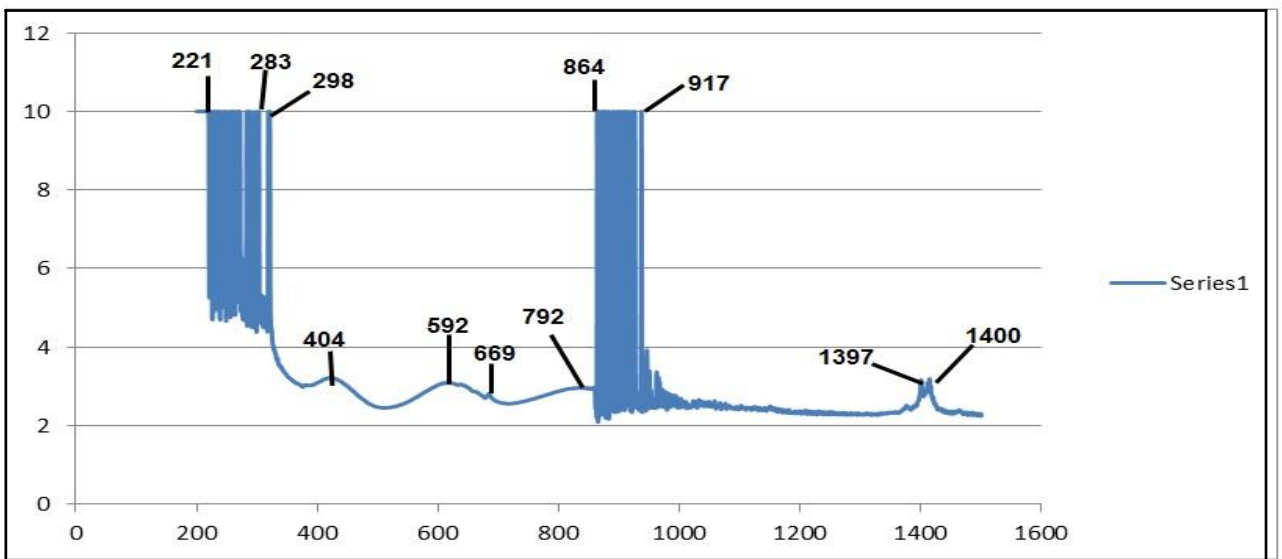
DSK-2 Fig 99
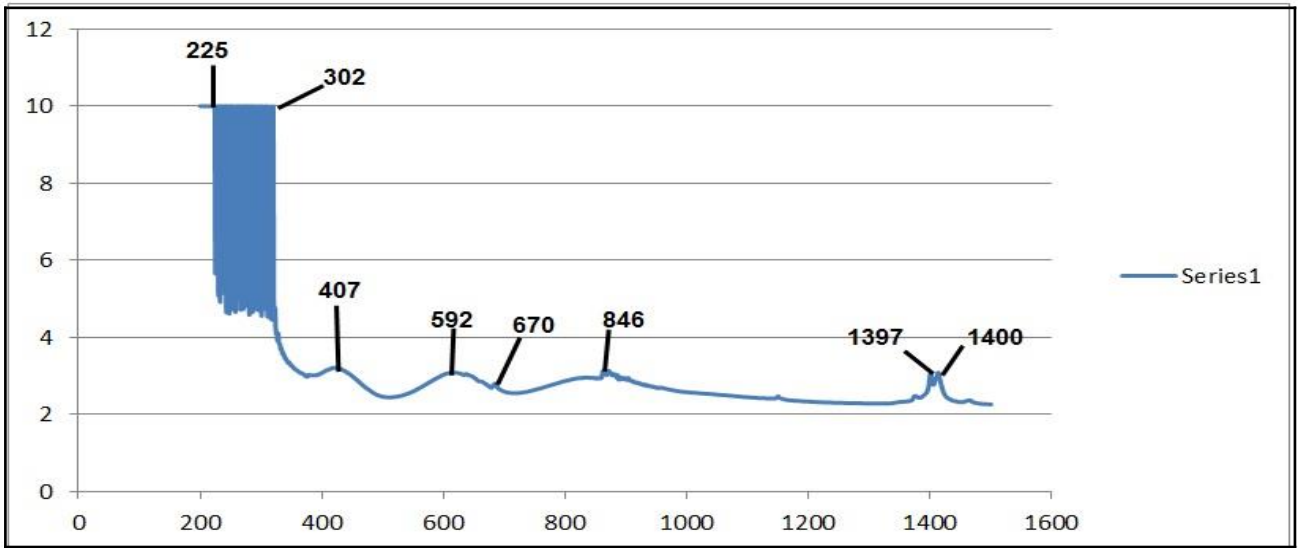
DSK 3 Fig 100
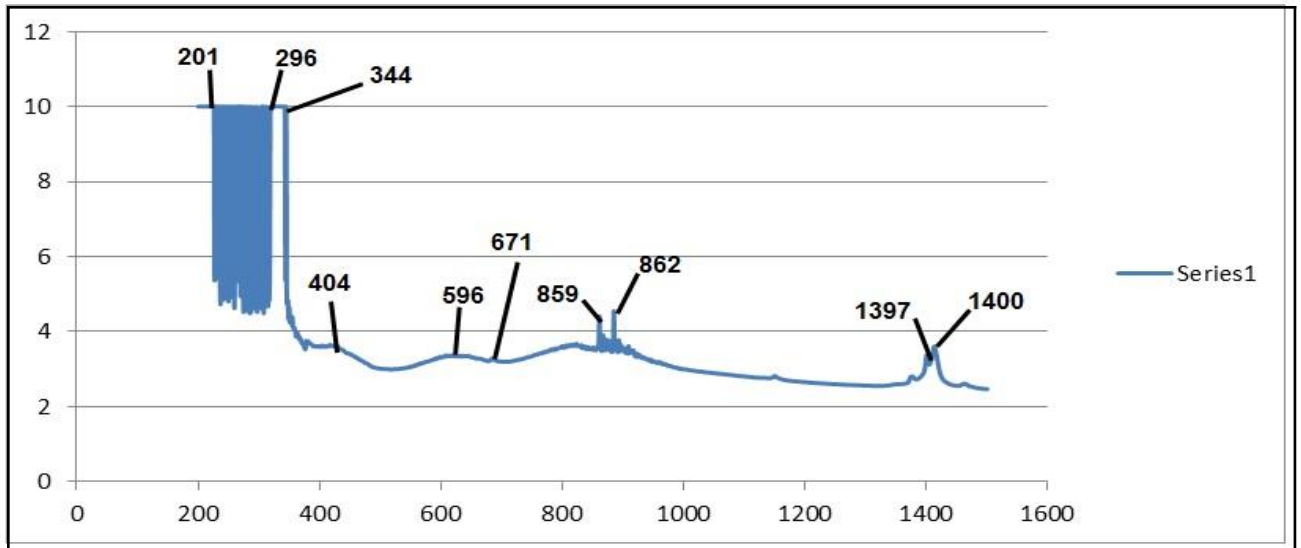
DSK 4 Fig 101
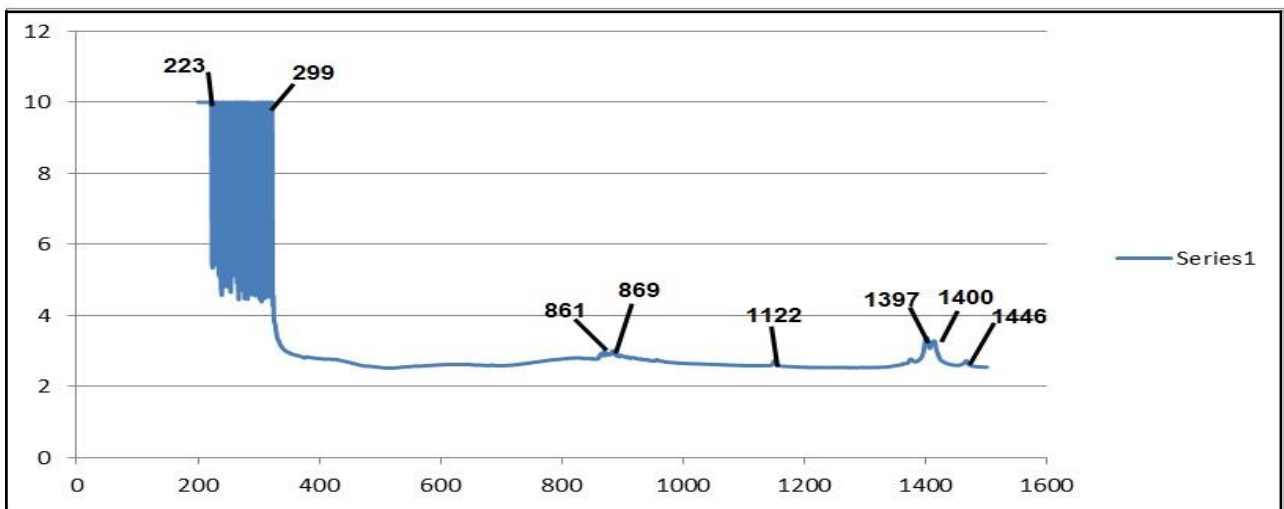
DSK 5 Fig 102
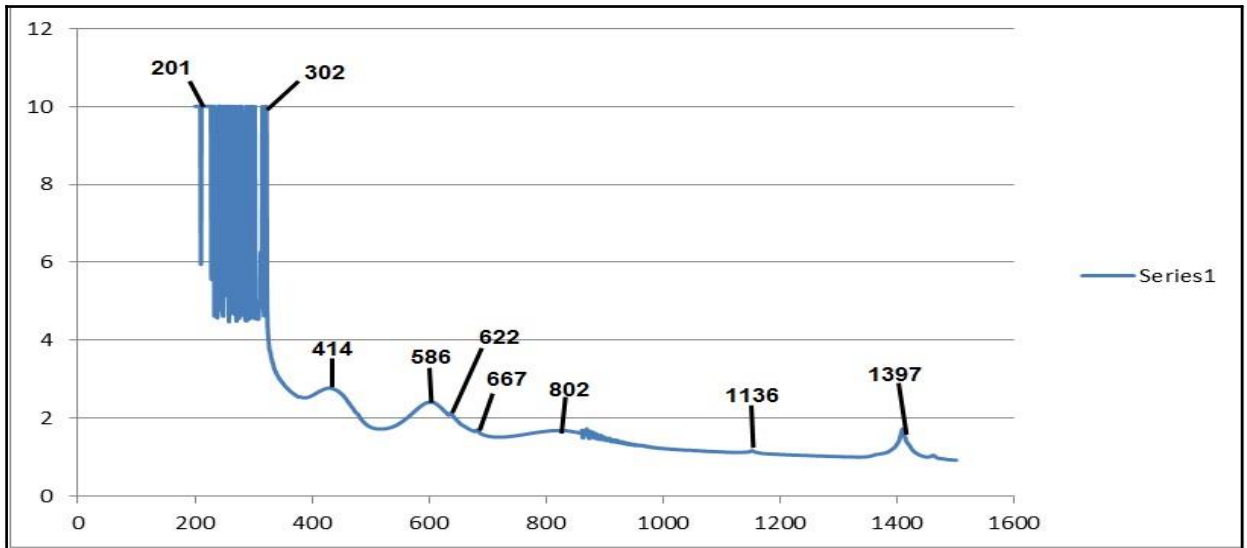
DSK 6 Fig 103
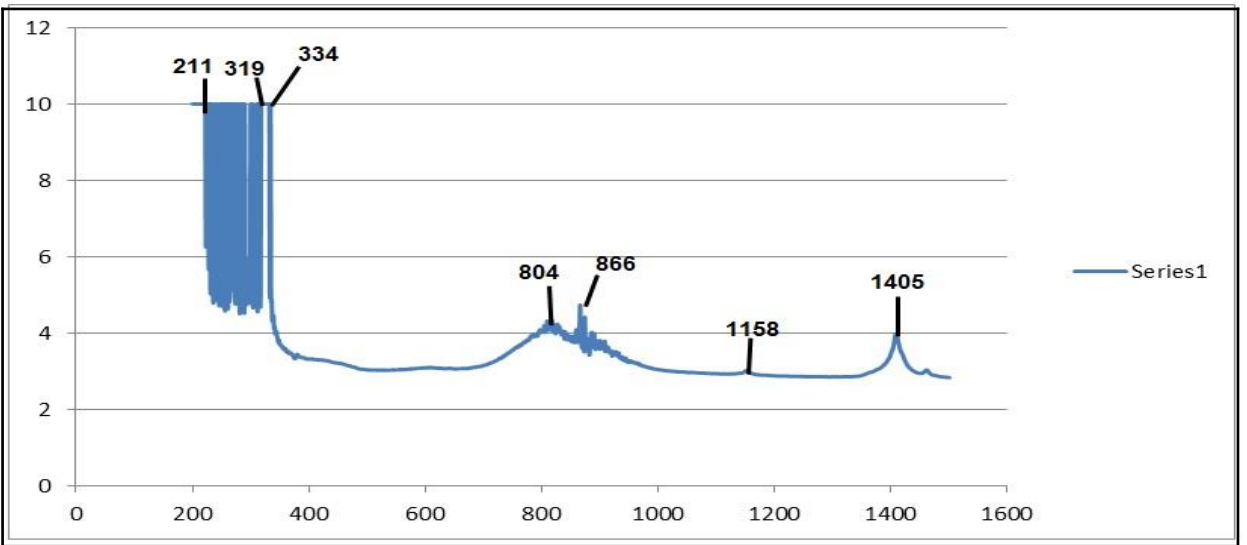
DSK 7 Fig 104
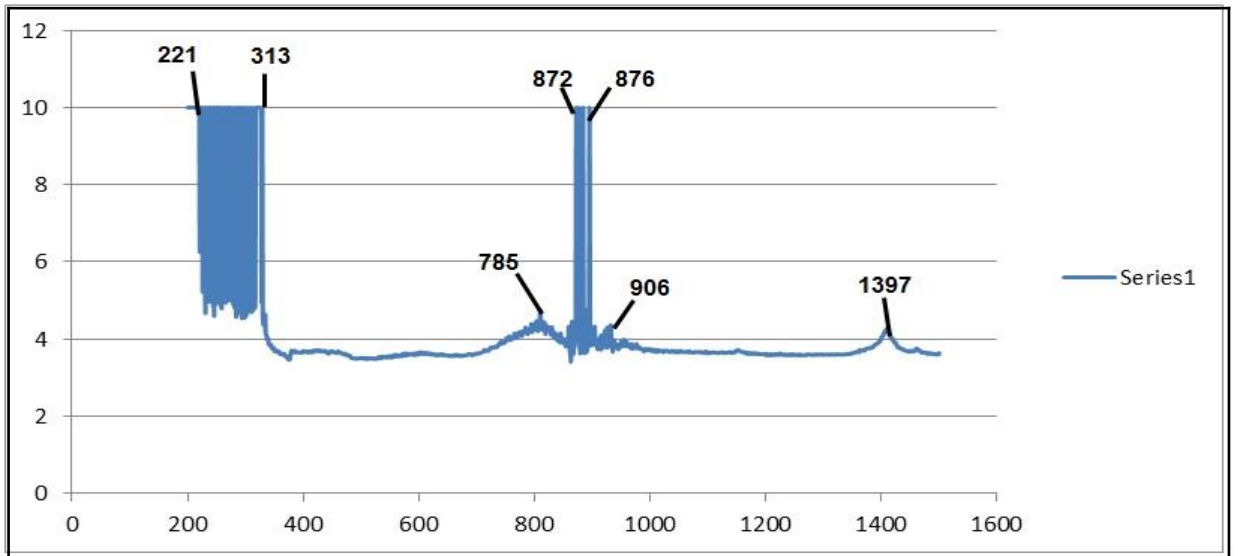
DSK 8 Fig 105
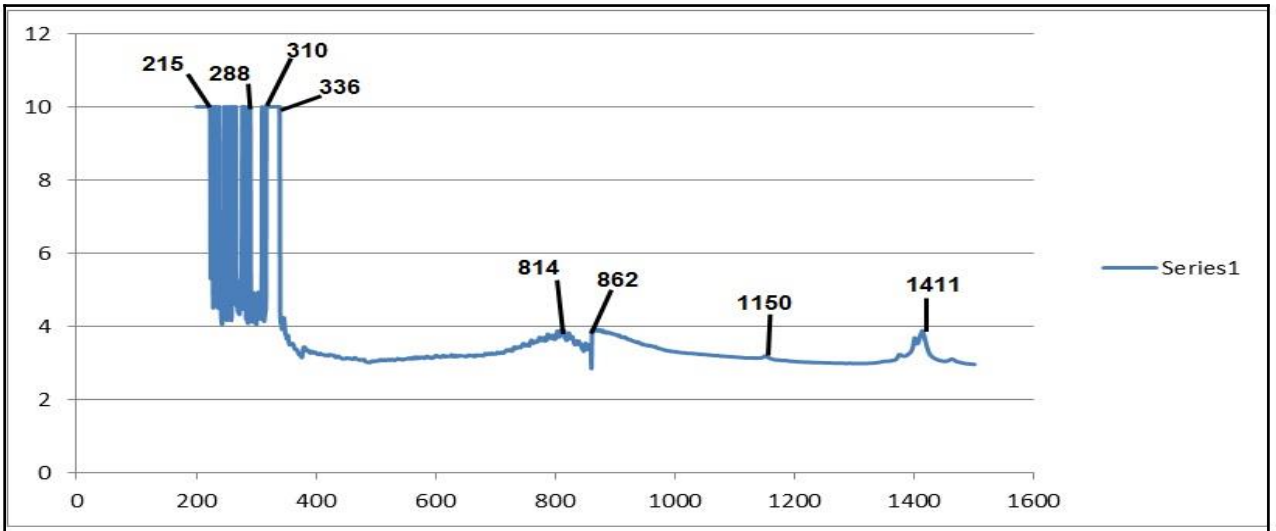
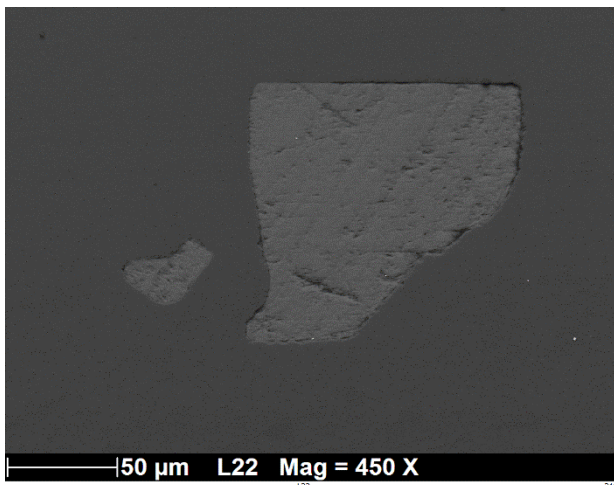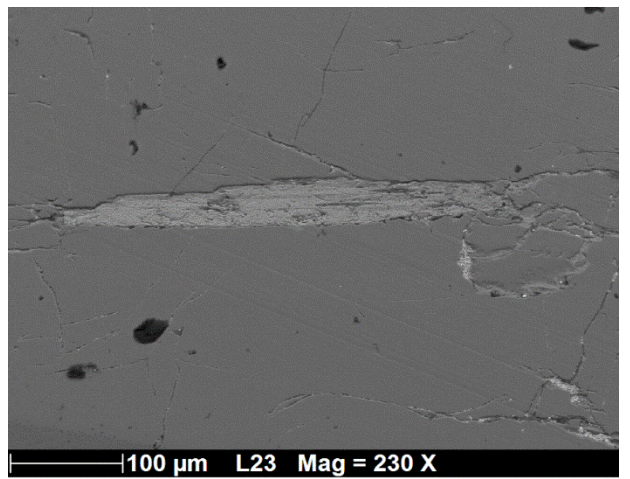

Scanning Electron Microscope (SME)
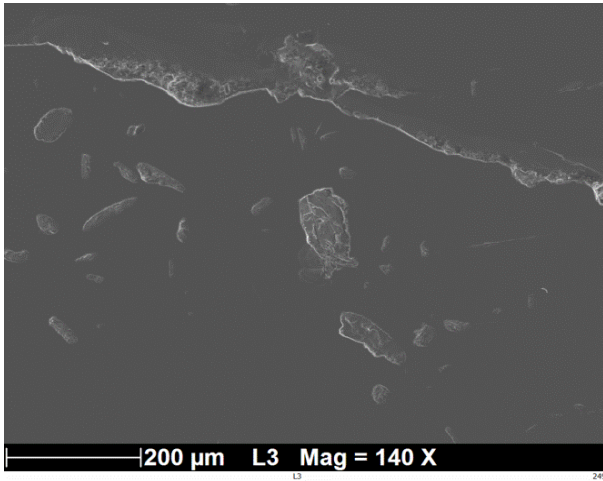
DSK-1 Fig 106
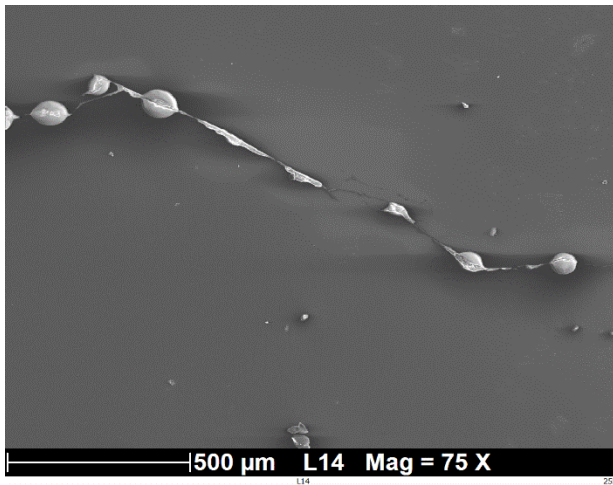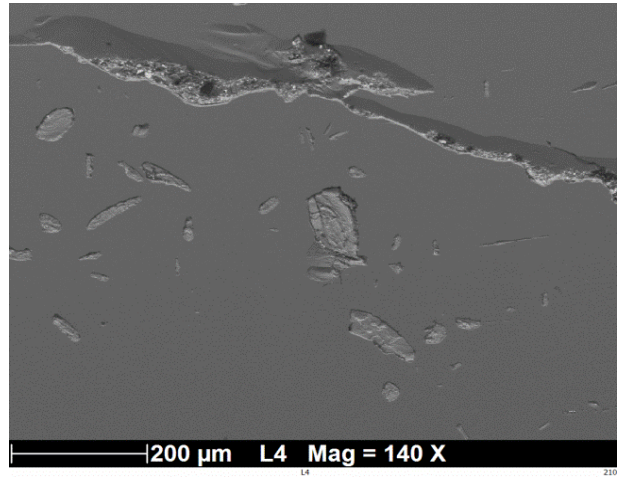

DSK-1 Fig 107
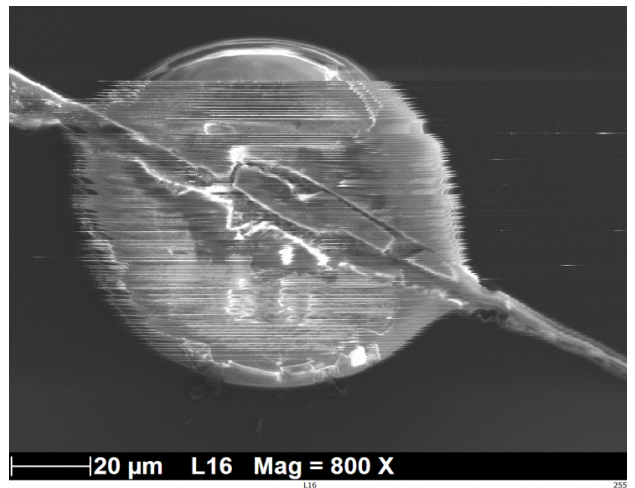
DSK-1 Fig 108

DSK-2 Fig 109

DSK-3 Fig 110
SE

200 µm   L3   Mag = 140 X

DSK-3 Fig 111
BSE

200 µm   L4   Mag = 140 X

DSK-6 Fig 112

50 µm   L2   Mag = 650 X

DSK-6 / SE Fig 113

200 µm   L0   Mag = 80 X

DSK-6 / BSE Fig 114

200 µm   L1   Mag = 80 X